



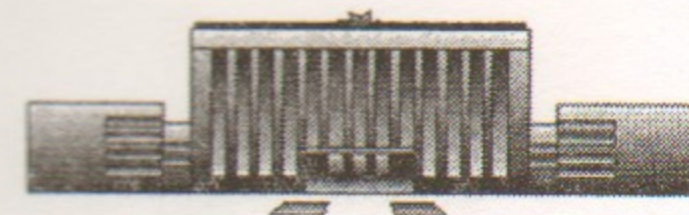
B.33  
1998

Budker Institute of Nuclear Physics  
SB RAS

B. Bayanov, V. Belov, A. Chernyakin,  
C. Crowford, S. O'Day, V. Eschenko, V. Karasyuk,  
M. Petrichenkov, Yu. Petrov, G. Silvestrov,  
T. Sokolova, T. Vsevolozhskaya

**LIQUID LITHIUM LENS  
FOR FERMILAB ANTIPROTON SOURCE**

Budker INP 98-23



Novosibirsk

## Liquid Lithium Lens for Fermilab Antiproton Source

B. Bayanov, V. Belov, A. Chernyakin,  
V. Eschenko, V. Karasyuk, M. Petrichenkov, Yu. Petrov,  
G. Silvestrov, T. Sokolova, T. Vsevolozhskaya

Budker Institute of Nuclear physics SB RAS  
630090 Novosibirsk, Russia

C. Crawford, S. O'Day

Fermi National Accelerator Laboratory

### ABSTRACT

The design of liquid lithium lens, developed at BINP, for antiprotons collection is performed. The design of the whole liquid lithium circuit, including lens, locking valves, pump and other elements is performed also. The procedure of system turn on and adjustment is considered. Some experimental data of measurements of lithium circuit parameters is given.

©Budker Institute of Nuclear Physics SB RAS

## CONTENTS

1. Introduction	5
2. Mechanical stresses in the lens	10
3. Heating	20
4. Liquid lithium lens design	25
5. A system for pumping of liquid lithium through a lens	30
5.1 The experimental measurements of hydrodynamical parameters of the lithium circuit	35
5.2 Hydrodynamic model of the lithium circuit	36
6. Liquid lithium pumps	37
6.1 Piston type pump	42
Magnetic system of liquid lithium pump	47
The power supply system of liquid lithium pump	51
6.2 Electromagnetic pump of spiral type	54
7. Lithium circuit cooling	57
8. Locking valves	61
9. Measures and adjustment of static pressure in lithium system.	66
10. Liquid lithium flow-meter	67
11. Layout of lithium system in antiproton target station	68
11.1 Lithium circuit protection	73
12. System heating and turn-on	74
References	77

# 1 INTRODUCTION

The lithium lens is a current carrying cylinder of lithium surrounded by a thin wall envelope, which turns at the ends into disks of bigger radius than that of the cylinder, thus providing axially symmetric current input. The envelope is made of titanium alloy VT-6 which has the highest specific resistance among other metals ( $\rho_{Ti} = 1.4 \cdot 10^{-4} \text{ Ohm} \cdot \text{cm}$ ), together with good mechanical characteristics and high corrosion resistance in lithium. Because of small thickness of envelope and high  $\rho_{Ti}$ , only a small part of full current is branched off to it. The lens is supplied by half sine wave current pulses with long enough duration to provide a homogeneous distribution of current density across the lithium cylinder at current pulse maximum. It results in linear growth of field with radius, which is necessary for aberrationless focussing of particles passing along the cylinder axis. Typical design of a lens with solid lithium and water cooling, developed for antiproton collection at BINP [1], FNAL [2] and CERN [3], are shown at Fig. 1(a,b) and Fig. 2. The BINP and FNAL lenses can be named the *elastic structures*. Their thin-wall titanium envelope expands freely with thermal expansion of lithium cylinder caused by pulsed heating. The CERN lens is rather a *rigid structure* because its envelope is supported by a big number of ceramic balls ( see Fig. 2 ), which restrict the radial size of envelope. Design of the lens with *liquid lithium*, now under development at BINP, is presented in Fig. 3. The removal of power released in the lens operating volume is realized by pumping of liquid lithium through the lens and the heat exchanger. The thin-wall titanium envelope in this design is covered by ceramic layer and is supported by a rigid thick-wall cylinder, which restricts the radial expansion.

The role of elastic element in this system plays the buffer volume of lithium, situated in peripheral part of lens in a region of axially symmetric current inputs ( Fig. 3 ). In addition, it is necessary to take into account that compressibility of liquid lithium is  $\approx 5$  times more than that of solid lithium. It absorbs the thermal expansion of heated lithium, thus decreasing the pulsed pressure in operating part of the lens.

In the lens with solid lithium also there is the buffer volume in current input region ( Fig. 1 a,b ), but at high pressure it operates efficiently only at low repetition rate because of a big time of relaxation of a stress, exceeding the elasticity limit in solid lithium. As it is shown experimentally in [4], the pressure, transferred to the buffer volume in result of thermal expansion of lithium in operating part of the lens, remains there for a time of the order of 1 min.

Thus, when the repetition rate is about 1 Hz, THE BUFFER VOLUME CAN NOT BE USED FOR DECREASING OF PULSED PRESSURE IN LENSES WITH SOLID LITHIUM.

Relaxation time of pressure in a lens with liquid lithium is of the order of sound propagation time through the system and does not limit the repetition rate.

An analysis of mechanical stresses, arising in lens from the pulsed magnetic field and thermal expansion of lithium, limiting the permissible field value and an efficiency for work, is performed below. This analysis gives the answer to a question: WHY SHOULD THE LITHIUM BE LIQUID?

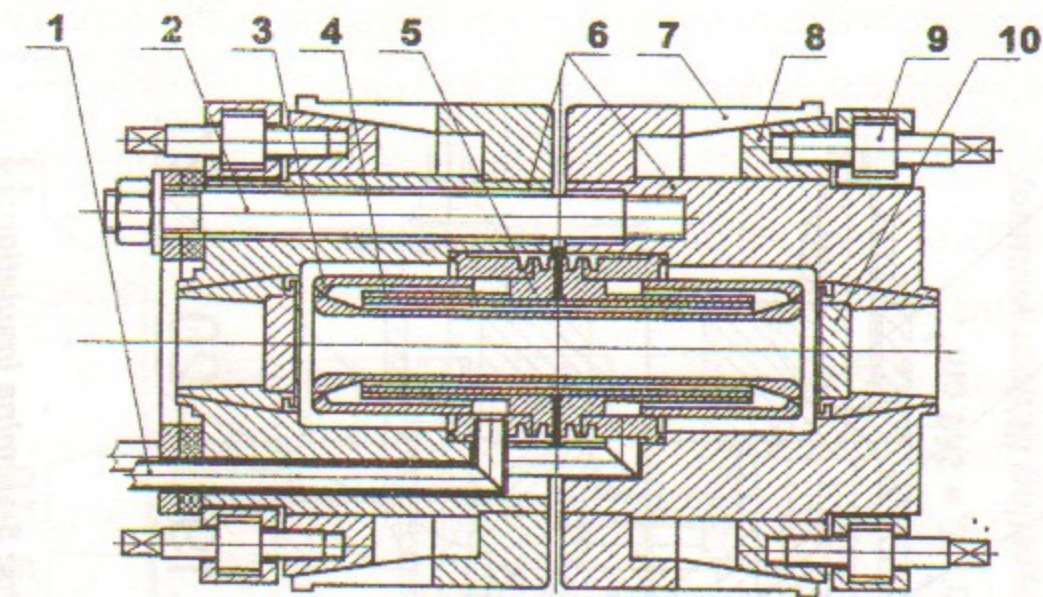


Fig.1a. BINP solid lithium lens with elastic wall.

1-water supply; 2-retaining bolts; 3-titanium body of the lens; 4-distribution pipes of the water system; 5-flanges of the distribution pipes; 6-steel body of the lens; 7-collecting contact; 8-conical clamps; 9-bolts; 10-berillium windows.

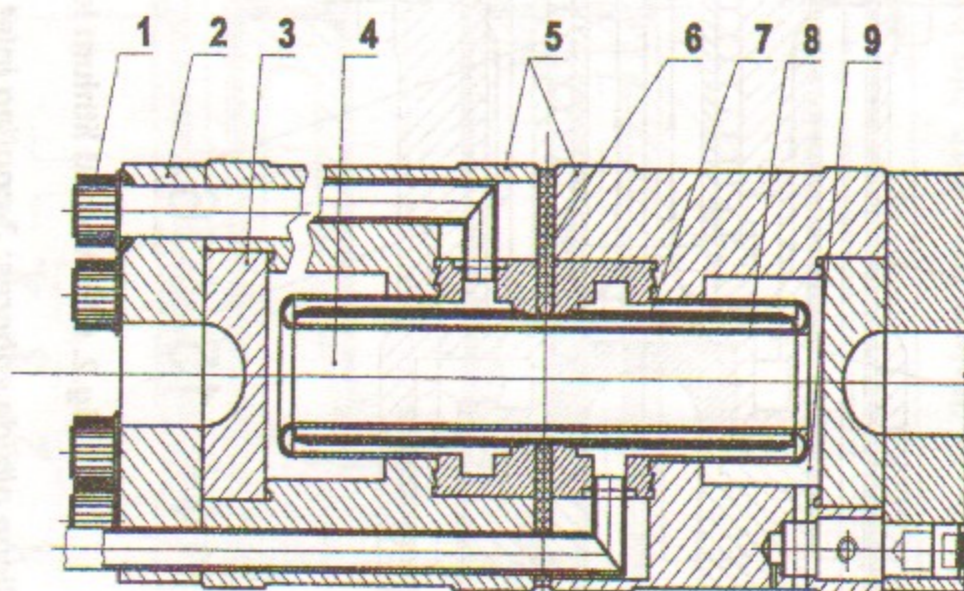


Fig.1b. FNAL solid lithium lens with elastic wall.

1-retaining bolt; 2-end flange; 3-end caps; 4-lithium; 5-current contacts; 6-ceramic insulator; 7-water septum; 8-inner cooling jacket; 9-fill port.

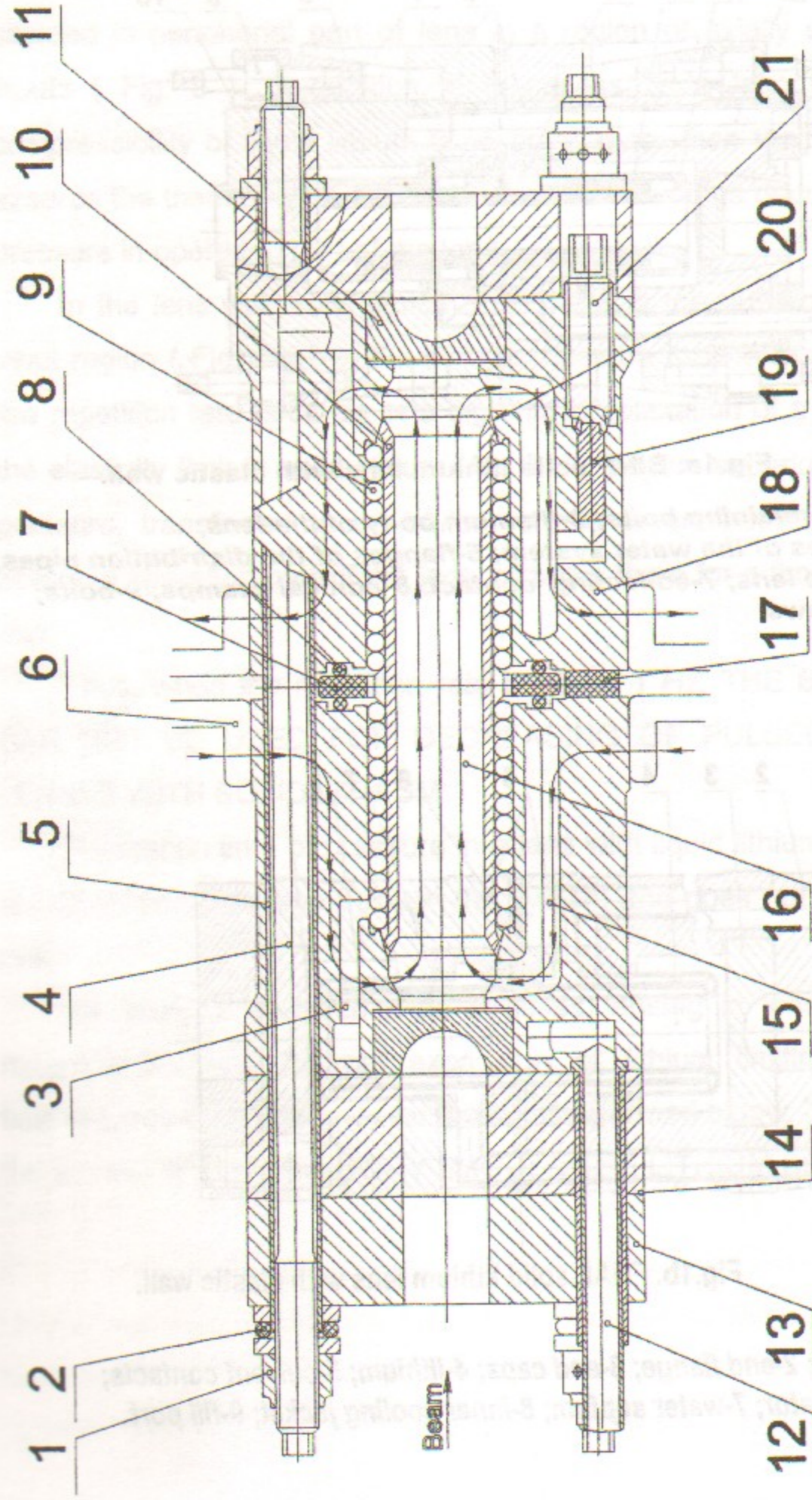


Fig. 2. CERN solid lithium lens with rigid envelope.

- 1-titanium nut; 2-silicon nitride spheres; 3-cooling inlet channels; 4-titanium tie bolts; 5-alumina insulation;
- 6-current contacts; 7-silicon nitride ring; 8-metal gaskets; 9-silicon nitride spheres; 10-stainless steel container;
- 11-titanium window; 12-cooling inlet pipe; 13-insulated auxiliary flange; 14-insulating mica disk; 15-lithium channels;
- 16-central lithium rod; 17-ceramic spacers; 18-steel housing; 19-pressure piston; 20-final weld after assembly;
- 21-sealing plug.

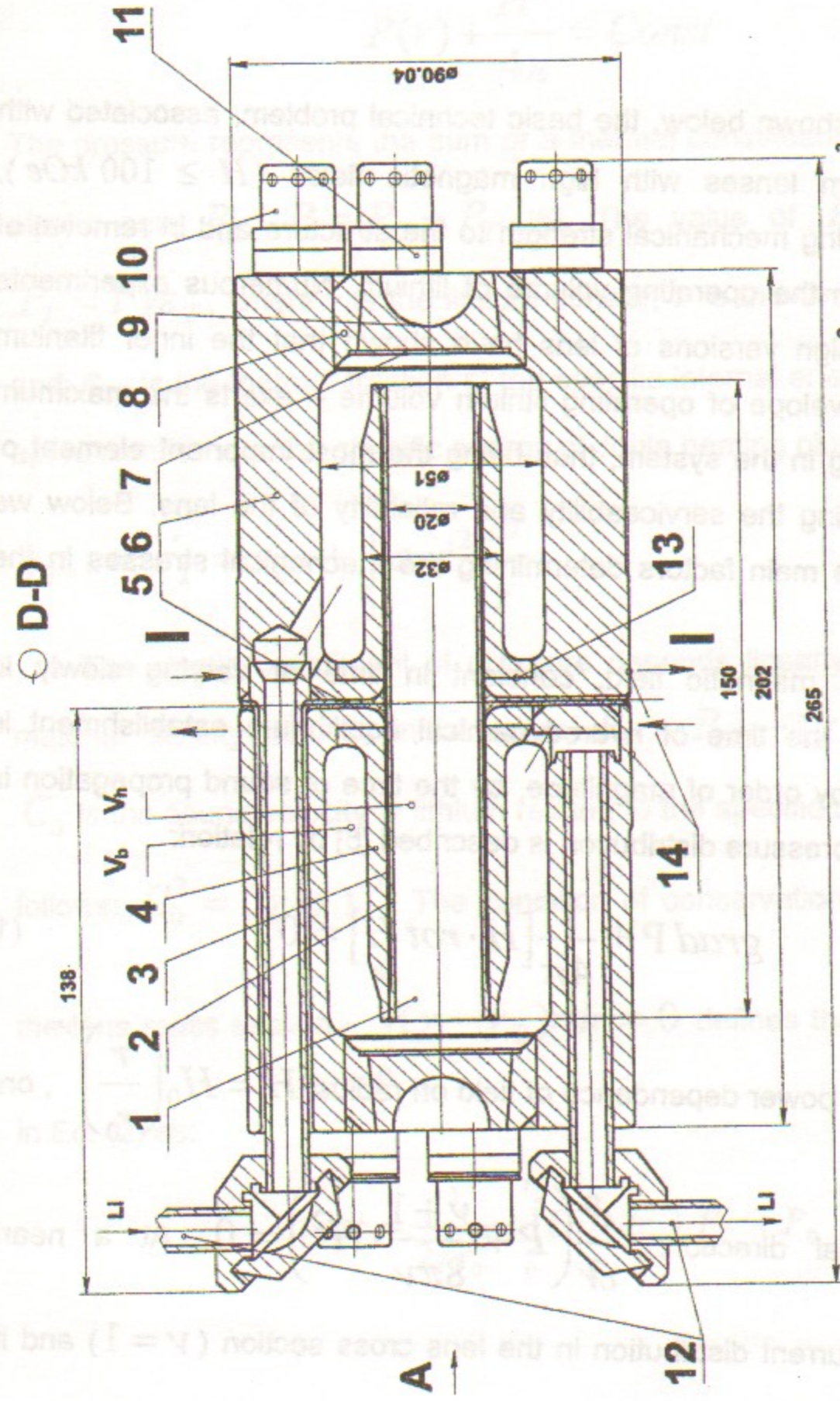


Fig. 3. Liquid lithium lens with big buffer volume:  $V_h = 53 \text{ cm}^3$ ,  $V_b = 240 \text{ cm}^3$ .

- 1- operating lithium volume; 2- thin-wall titanium envelope of the operating lithium volume;
- 3- separating ceramics insulators; 4- thick-wall titanium cylinder; 5- face ceramics insulator;
- 6- stainless steel lens body; 7- protective titanium foil; 8- cylindrical stainless steel details;
- 9- beryllium inserts; 10- retaining bolts; 11- insulating washers; 12- supplying tubes for liquid lithium.
- 13 - place of stainless steel-titanium thermomdiffusion welding 14-places of current input

## 2 MECHANICAL STRESSES IN THE LENS

As it will be shown below, the basic technical problem, associated with creation of lithium lenses with high magnetic fields ( $H \geq 100 \text{ kOe}$ ), consists of providing mechanical strength to the structure and in removal of power released in the operating volume of lithium. Numerous experiments with different design versions of lens have shown that the inner titanium cylinder – the envelope of operating lithium volume – exerts the maximum stresses occurring in the system, thus being the most important element of system, determining the serviceability and reliability of the lens. Below we shall consider the main factors determining the mechanical stresses in the lens.

In presence of magnetic field, constant in time or varying slowly in comparison with the time of hydrodynamical equilibrium establishment in lithium (defined, by order of magnitude, by the time of sound propagation in the system), the pressure distribution is described [5] by relation:

$$\text{grad } P + \frac{1}{4\pi} [H \cdot \text{rot } H] = 0 \quad (1)$$

Assuming a power dependence of field on radius  $H = H_0 \left( \frac{r}{r_0} \right)^\nu$ , one

obtains in radial direction:  $\frac{\partial}{\partial r} \left( P + \frac{\nu+1}{8\pi\nu} \cdot H^2 \right) = 0$ . At a nearly

homogeneous current distribution in the lens cross section ( $\nu = 1$ ) and its

length, much larger than the radius, the pressure in the central part of the lens is dependent on radius as:

$$P(r) + \frac{H^2}{4\pi} = \text{Const} \quad (2)$$

The pressure represents the sum of a thermal constituent  $P_T$  and a "cold" elastic one  $P_C$ :  $P = P_C + P_T$  [6]. The value of  $P_T$  is defined as,

$P_T = \Gamma \gamma \varepsilon_T$ , where  $\gamma$  is the lithium density,  $\Gamma$  is the Gruneisen coefficient,

and  $\varepsilon_T$  is the thermal fraction of the specific internal energy, equal – in first approximation – to the specific energy of Joule heating plus the initial value of

$$\varepsilon_T, \text{ i. e. } \varepsilon_T = \varepsilon_{0T} + \int_0^t \rho \cdot j^2 \frac{dt}{\gamma}$$

The elastic constituent of pressure depends linearly on a deviation of material density from its initial value:  $P_C = P_{0C} + (\gamma - \gamma_0) C_0$ , where

$C_0$  is the sound velocity in lithium related to the specific compressibility  $\chi$  as

follows:  $C_0^2 = (\chi \cdot \gamma)^{-1}$ . The condition of conservation of lithium mass in

the lens cross section,  $\int_0^{r_0} (\gamma - \gamma_0) r dr = 0$  defines the value of constant

in Eq. (2) as:

$$\text{Const} = \frac{1}{2\pi r_0^2} \cdot \int_0^{r_0} H^2 r dr + P_T + P_0 \quad (3)$$

Here  $P_0$  is the full initial pressure, while the above  $P_{0C}$  is its elastic constituent. Under normal initial conditions the values of  $P_0$ ,  $P_{0C}$  and  $\varepsilon_{0T}$  as well as  $P_{0T} = \Gamma \gamma_0 \cdot \varepsilon_{0T}$  may be assumed to be zero. If a preliminary compression is given in the system, the non-zero value of  $P_0$  arises on account of the non-zero  $P_{0C}$ , while the value of  $P_{0T}$  remains zero.

Making allowance for time dependence of the field  $H \propto \sin \omega t$ , and of the Joule heating  $\varepsilon_T \propto \int \sin^2 \omega t dt$ , one obtains the pressure distribution over the lens cross section – by a fairly large thickness of skin-layer  $\delta$ ,  $\delta \geq 0.7$ , in a form:

$$P(r) = P_0 + \frac{\Gamma H_0^2}{4\pi} \left(\frac{\delta}{r_0}\right)^2 \cdot \left(\omega t - \frac{\sin 2\omega t}{2}\right) + \frac{H_0^2}{8\pi} \cdot \left(1 - 2\frac{r^2}{r_0^2}\right) \cdot \sin^2 \omega t \quad (4)$$

The thermal constituent  $P_T$  is defined by the second term of expression (4). Taking into account that the Gruneisen coefficient is expressed through the coefficient of thermal expansion  $\alpha$ , specific heat capacity  $C_v$ , specific compressibility and density as  $\Gamma = \frac{\alpha}{\gamma \chi C_v}$ , this term is

reduced to the form

$$P_T = \frac{\alpha T}{\pi \chi} \left(\omega t - \frac{\sin 2\omega t}{2}\right), \text{ where } T = \frac{H_0^2 \delta^2}{4\gamma C_v r_0^2} \text{ is the temperature}$$

of heating for the half sine wave current pulse, homogeneous over the lens cross section in the case  $\delta \geq 0.7$ .

At smaller values of  $\delta/r_0$  the pressure, caused by heating, is defined by a temperature  $\bar{T}(r)$  average over the cross section. Here this pressure is not already a purely thermal constituent, but includes the elastic one, associated with the redistribution of lithium density across the lens to compensate the inhomogeneity of  $P_T$  due to the heating inhomogeneity.

The third term in eq. (4) describes an influence of the magnetic field.

The former leads to unloading by the quantity  $-\Delta P = \frac{H_0^2}{8\pi}$  on the surface of lithium cylinder, and to an additional loading by the same quantity on the axis.

The minimum value of pressure on the surface is achieved in a phase

$$\omega t = \text{arctg} \frac{r_0^2}{2\Gamma \delta^2}. \text{ With } \delta/r_0 = 0.7 \text{ one obtains } \text{tg} \omega t = \frac{1}{\Gamma} \text{ and}$$

$$P_{\min}(r_0) = P_0 + \frac{H_0^2}{8\pi} \cdot (\Gamma \cdot \text{tg} \Gamma - 1). \text{ Substituting } \Gamma = \frac{\alpha}{\chi \Gamma C_v} \cong 1 \text{ in}$$

lithium, we find that  $\omega t \cong \frac{\pi}{4}$  and  $P_{\min}(r_0) = P_0 - 0.21 \frac{H_0^2}{8\pi}$ .

At close to zero initial pressure,  $P_0 \cong 0$  the value of  $P_{\min}(r_0)$  proves to be negative. This means that the lithium cylinder has to be radially compressed by the quantity  $\Delta r$ , such that the pressure arising in lithium compensates the negative value of  $P_{\min}$  on the surface, i.e.

$$(\bar{P}_{end})_{max} = \frac{\Gamma H_0^2}{4\pi} \left(\frac{\delta}{r_0}\right)^2 \cdot \bar{\omega t} + \frac{H_0^2}{8\pi}$$

At  $\delta/r_0$  this implies that  $\bar{\omega t} = 154$  and  $(\bar{P}_{end})_{max} = P_0 + 3.2 \frac{H_0^2}{8\pi}$ ,

which only slightly differs from the value  $(\bar{P}_{end}) = P_0 + \frac{H_0^2}{8}$  in the phase  $\bar{\omega t} = \pi$

The preceding consideration of pressure in an absolutely rigid structure defines the upper limit of pressure, obtained in real structures. In real cases there always are some elastic elements, which take upon themselves the thermal expansion of the operating lithium volume, thus being similar to a specific "buffer".

The titanium envelope of lithium cylinder in the structures under consideration serves as one of the basic elastic elements, the other of which is the lithium in the edge regions and in those of current-inputs, where the lithium is heated considerably less than in the operating volume. Neglecting the finite elasticity of other elements of structure and the heating of lithium in the "buffer" volume, let us find the pressure in the system and the stress in the envelope at the end of current pulse, when the temperature and pressure are maximum.

The radial extension of envelope under a pressure of heated lithium gives rise to the stress  $\sigma = E \frac{dR}{R}$  in its wall, defined by the elasticity

modulus of titanium  $E$  and the relative increment of envelope radius. By that the operating lithium volume  $V_0$  gets an expansion  $dV_R = 2\pi l R dR$

( $l$  stands for the lens length), which results in reduction of pressure in it by a

$$\text{magnitude } dP_R = -\frac{1}{\chi} \frac{dV_R}{V_0} = -\frac{2}{\chi} \frac{dR}{R}$$

Transfer of pressure to the "buffer" lithium volume  $V_b$  results in compression of the buffer lithium volume by  $dV_b$  and in the equal expansion of the operating volume. This also reduces the pressure in the

latter by  $dP_b = -\frac{1}{\chi} \frac{dV_b}{V_0}$ . The total pressure in the operating volume,

$$P = P_T + dP_R + dP_b, \text{ where } P_T = \frac{\alpha T}{\chi}, \text{ should be equal to the pressure}$$

in the buffer volume  $P_b = \frac{1}{\chi} \frac{dV_b}{V_b}$ , and connected with the stress in the

envelope wall by the relation  $P = \sigma \frac{\Delta}{R}$ , where  $\Delta$  is the wall thickness. The

resulting set of equations reads:

$$\sigma = E \frac{dR}{R}, \quad P = \sigma \frac{\Delta}{R}, \quad P_b = \frac{1}{\chi} \frac{dV_b}{V_b}, \quad P = P_b$$

$$P = P_T - \frac{1}{\chi} \left( 2 \frac{dR}{R} + \frac{dV_b}{V_0} \right)$$

Its solution defines the value of  $\sigma$  versus the temperature and design parameters of the lens as follows:



$$\sigma = \frac{\alpha T}{\chi_{Li} \frac{\Delta}{R} \left(1 + \frac{V_b}{V_0}\right) + \frac{2}{E_{Ti}}}$$

and the pressure in the system as:

$$P = \frac{\alpha T}{\chi_{Li} \left(1 + \frac{V_b}{V_0}\right) + \frac{R}{\Delta} \cdot \frac{2}{E_{Ti}}}$$

In a rigid structure, such as the CERN lens (fig. 2), the pressure will achieve its maximum value  $P = \frac{\alpha T}{\chi}$ , which by the compressibility of solid

lithium  $\chi_{sol} = 9.1 \cdot 10^{-6} \text{ atm}^{-1}$ , by  $\alpha = 1.8 \cdot 10^{-4}$ , and temperature  $T = 60$ , corresponding to  $H_0 = 100 \text{ kOe}$ , means  $P = 1200 \text{ atm}$ . In

lenses with elastic envelope (Fig. 1 a,b) by  $\frac{\Delta}{R} = 0.1$ , the pressure will be equal to  $P \approx 370 \text{ atm}$ , however the mechanical stress in the titanium

envelope, equal  $\sigma \approx 3700 \frac{\text{kg}}{\text{cm}^2}$ , does practically achieve the limit value for

millions cycles operation  $\sigma^{-1} \approx 4000 \frac{\text{kg}}{\text{cm}^2}$ .

In a liquid lithium structure now under consideration, with  $\frac{R}{\Delta} \approx 1$  and compressibility  $\chi_{liq} = 5 \cdot 10^{-5} \text{ atm}^{-1}$ , the second term in the denominator does not much effect the pressure, which may be expressed as:

$$P = \frac{\alpha T}{\chi_{liq} \left(1 + \frac{V_b}{V_0}\right)}$$

With conserved ratio  $\delta/R \approx 0.7$ , which by higher specific resistance in liquid lithium is achieved by the less pulse duration, the pulsed heating temperature is also conserved, being equal to  $T = 60$  for

$H_0 = 100 \text{ kOe}$ . In geometry of Fig. 3  $\frac{V_b}{V_0} = 4.5$ , and the pressure appears equal to  $40 \text{ atm}$ .

So, IN SYSTEMS WITH LIQUID LITHIUM THE PRESSURE, CAUSED BY THE PULSED HEATING, CEASES TO BE THE MAIN FACTOR, DETERMINING THE RELIABILITY OF LENS OPERATION.

Besides that the transition from the water cooling with heat removal through the envelope of titanium, whose thermo-conductivity is rather low, to the pumping of liquid lithium through the lens and the heatexchanger, TAKES OFF THE RESTRICTION OF REPETITION RATE, which now is defined only by a power of pumping system.

It is the fundamental advantage of system with liquid lithium. But there are some negative results of passing to liquid lithium – the possible need to increase static pressure in the system – preload up to  $300 \text{ atm}$ . It leads to

complication of the liquid lithium pumping system and determines the choice of type and design of pump which pumps out liquid lithium.

Directly at the lens the radial component of this static pressure is applied to the thick-wall body of the lens (6 in Fig. 3), The axial one acts on the lens face with berillium inserts. (9 in Fig. 3)

The next source of mechanical stresses in the lens is the pulsed pressure from magnetic field in current inputs which is applied in the insulating gap to two halves of lens body and transmits to retaining bolts (10 in Fig. 3)

Full magnetic field force passing to the bolts is expressed as:

$$F_M = P_M \cdot 2\pi \ln \frac{r_2}{r_1}$$

where  $P_M$  - magnetic field pressure at radius  $r_1 = 1.15 \text{ cm}$  corresponding to the surface of ceramics that covers the inner cylindrical envelope,  $r_2$  - outer diameter of the lens body, where the current contact is performed. In geometry of Fig.3 ( $r_2 = 4.5 \text{ cm}$ ) at magnetic field  $H_{\max} = 10 \text{ T}$   $F_M = 3427 \text{ kG}$  and at  $H_{\max} = 13 \text{ T}$   $F_M = 5792 \text{ kG}$ .

### 3 HEATING

By supplying the lens with the half-sine wave current pulses,

$$I(t) = I_0 \sin \omega t, \quad 0 \leq t \leq \frac{\pi}{\omega},$$

the distribution of temperature of heating for a pulse over the radius in lithium cylinder is defined as follows [7]:

$$T(r) = \frac{1}{8\pi\gamma C_v} \left\{ \pi H_0^2 \left| \frac{J_0(x\sqrt{i})}{J_1(x_0\sqrt{i})} \right|^2 + 4 \sum_{l=1}^{\infty} \sum_j^{\infty} \frac{a_j b_l \mu_j \mu_l}{\mu_j^2 + \mu_l^2} J_0(\mu_j r) J_0(\mu_l r) - \right. \\ \left. - 2 \sum_{j=1}^{\infty} a_j b_j J_0(\mu_j r) J_0(\mu_j r_0) \operatorname{Re} \left[ \left( 1 + \frac{i\mu_j^2 \delta^2}{2} \right) \frac{x_0 \sqrt{i} \cdot J_0(x\sqrt{i})}{J_1(x_0 \sqrt{i})} \right] \right\} \quad (8)$$

Here  $J_\nu(z)$  are the Bessel functions of  $\nu$  order,  $x$  and  $x_0$  are the ratios  $\frac{r\sqrt{2}}{\delta}$  and  $\frac{r_0\sqrt{2}}{\delta}$ ,  $\delta = c/\sqrt{2\pi\sigma\omega}$  is the skin depth, and  $\mu_j r_0$  are the roots of equation  $J_1(x) = 0$ , equal to 3.38, 7.02, 10.17, at  $j = 1, 2, 3, \dots$ , respectively,  $\lambda_j = \frac{\mu_j^2 \delta^2 \omega}{2}$ .

The coefficients  $a_j$  and  $b_j$  are found as [7]

$$a_j = -H_0 \left( \frac{\delta}{r_0} \right)^2 \frac{\mu_j r_0}{\left( 1 + \frac{\mu_j^4 \delta^4}{4} \right) J_0(\mu_j r_0)}, \quad b_j = a_j \left( 1 + e^{-\lambda_j \frac{\pi}{\omega}} \right)$$

They are the amplitudes of the relaxation constituents of magnetic field:

$$H(r,t) = H_0 \operatorname{Re} \left[ i \frac{J_1(x\sqrt{i})}{J_1(x_0\sqrt{i})} e^{-i\alpha t} \right] + \sum_{j=1}^{\infty} a_j J_1(\mu_j r) e^{-\lambda_j t}, \quad 0 \leq t \leq \frac{\pi}{\omega}$$

$$= \sum_{j=1}^{\infty} b_j J_1(\mu_j r) e^{-\lambda_j (t - \frac{\pi}{\omega})}, \quad t \geq \frac{\pi}{\omega}$$

which provide continuity over time in the current pulse over all the lens cross section. The constants  $\gamma$  and  $C_v$  are, respectively, the density and heat capacity of lithium,  $H_0$  is the field amplitude at the cylinder surface.

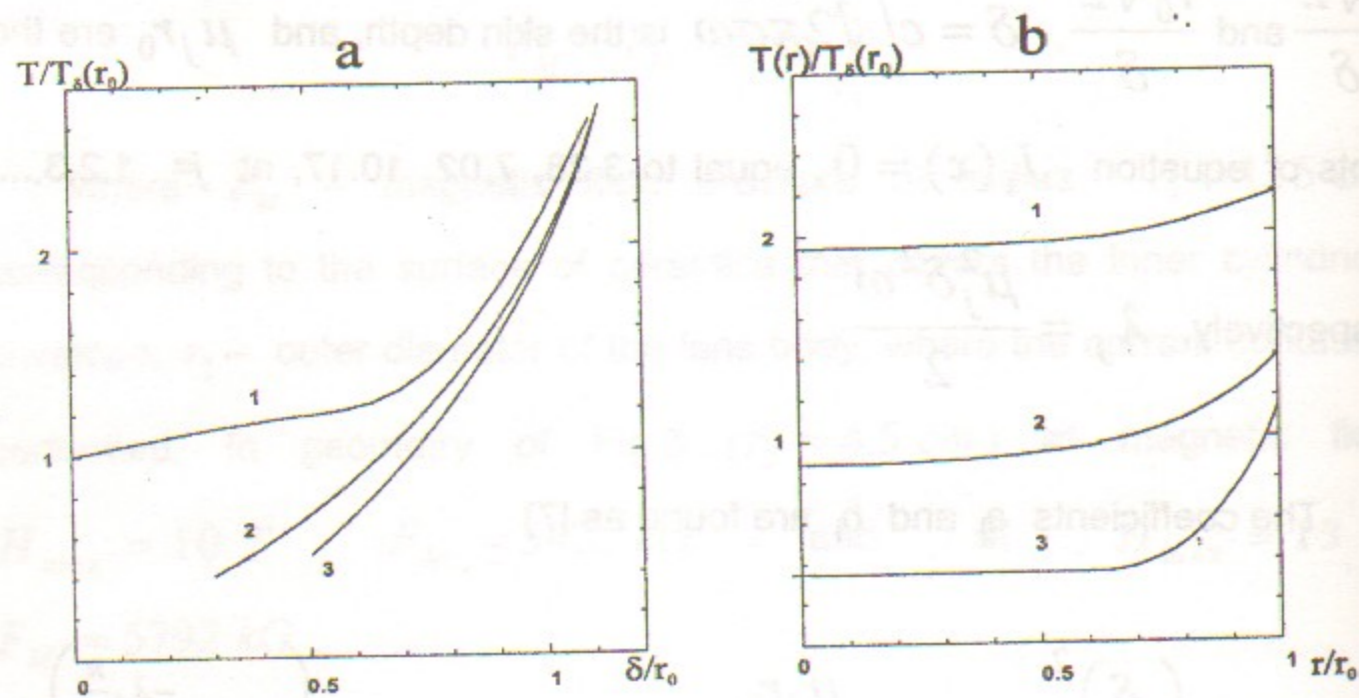


Fig. 4.

a: temperature of the lens in units of  $T_d$  versus  $d/r_0$ . 1 - temperature of the lens surface; 2 - temperature average over the lens cross-section by inhomogeneous current density distribution; 3 - homogeneous current density distribution.

b: temperature distribution versus  $r/r_0$  at different value  $d/r$ . 1-  $d/r=1$ ; 2-  $d/r=0.7$ ; 3-  $d/r=0.5$ .

The average temperature over the lens cross section is found equal to

$$\overline{T(r)} = \frac{H_0^2}{4\gamma C_v} \left( \frac{\delta}{r_0} \right)^2 \left[ 1 + \sum_{j=1}^{\infty} \frac{1}{1 + \frac{\mu_j^4 \delta^4}{4}} - \frac{1}{\pi} \sum_{j=1}^{\infty} \frac{\mu_j^2 \delta^2 \left( 1 + e^{-\mu_j^2 \delta^2 \frac{\pi}{2}} \right)}{\left( 1 + \frac{\mu_j^4 \delta^4}{4} \right)} \right] \quad (9)$$

It is seen from above formula, that the temperature dependence on pulse duration and specific resistance of material manifests itself through the dependence on the ratio  $\delta/r_0$  only. Owing to that, and because the temperature on the surface at  $\delta/r_0 \ll 1$ ,  $T_\delta$ , is independent of pulse

duration,  $T_\delta = \frac{H_0^2}{8\gamma C}$ , we characterise the heating by its analyses in

dependence on  $\delta/r_0$  only, and express the temperature in units of  $T_\delta$ . For lithium  $T_\delta = 60^\circ C$  for a field at the surface  $H_0 = 100 kOe$ .

In Fig. 4 there are presented: a - the temperature at the surface and the temperature average over the cross-section one versus the  $\delta/r_0$ , and b - the temperature distribution over the radial coordinate for different  $\delta/r_0$  [8].

As it follows from the figure, the independence of temperature at the lens surface on pulse duration, evident at  $\delta \ll r_0$ , is really observed up to  $\delta/r_0 \approx 0.5$ , which makes it unreasonable to reduce the pulse duration below this limit.

The dependence of temperature average over the cross-section on  $\delta/r_0$  at  $\delta/r_0 > 0.5$  is mainly described by the coefficient  $(\delta/r_0)^2$ , which means the linear dependence on pulse duration,  $\overline{T(r)} \propto \tau$ . The effect of current distribution inhomogeneity, defined by the expression in square brackets in (9), at  $\delta/r_0 = 0.7$  gives an increase of  $\overline{T(r)}$  by 1.08 times only. This permits to define the average temperature at  $\delta/r_0 \geq 0.5$  as

$$\overline{T(r)} \cong T_0 = \frac{H_0^2}{8\pi} \left( \frac{\delta}{r_0} \right)^2.$$

For  $\delta/r_0 = 1$  this value is  $T_0(\text{grad}) = 1.2 \cdot 10^{-8} H_0^2 (\text{Oe})$ , that is by 2 times higher than the temperature on the surface in skin regime  $T_s$ . At  $\delta/r_0 = 0.7$  the overheating does not exceed 10 %

In liquid lithium the specific resistance is described in dependence on temperature by an expression  $\rho = 27.9(1 + 2.7 \cdot 10^{-3} T) \mu\text{Ohm} \cdot \text{cm}$ .

At an average temperature  $T_{Li} \approx 250^\circ\text{C}$ , this means  $\rho = 48 \mu\text{Ohm} \cdot \text{cm}$ , which by more than 3 times exceeds the value below the melting point. To conserve the ratio  $\delta/r_0 \leq 0.7$  one needs to decrease the pulse duration in accordance with relation  $\delta(\text{cm}) = x\sqrt{\tau(\text{s})}$ . In our geometry, with  $r_0 = 1 \text{ cm}$ , the lens is to be supplied by current pulses of  $\tau = 300 \mu\text{s}$  duration.

#### 4 LIQUID LITHIUM LENS DESIGN

Let us discuss the lens design shown in Fig. 3, chapter 2 and in Fig. 5 a,b performed below.

The lens, itself, is a lithium cylinder ( in Fig. 3 ) surrounded by thin-wall titanium envelope (2).

Since liquid lithium has a big specific resistance ( $\rho_{liq} = 45 \cdot 10^{-6} \Omega \cdot \text{cm}$ ) the envelope is made of titanium alloy VT-6

with high specific resistance  $\rho_{Ti} = 140 \cdot 10^{-6} \Omega \cdot \text{cm}$  and has a wall thickness 1 mm. Thus only the small part of full current is branched off to it:

$$\frac{J_{Ti}}{J_{Li}} = \frac{2\Delta}{R} \cdot \rho_{Li} / \rho_{Ti}$$

here  $\Delta$  is the thickness of envelope,  $R$  – radius of cylinder.

The surface of this thin-wall cylinder is covered by ceramic layer of 0.5 mm thickness by means of detonation-gas method developed in the Institute of Hydrodynamics of Siberian Branch of Russian Academy of Sciences. Two thick-wall titanium cylinders (4) are put on ceramics coated thin-wall cylinder. This facilitates the reliable electron-beam welding of homogeneous metals at the faces of cylinder. This face welding is realized after preliminary welding of thick-wall cylinders (4) with lens body (6) made of stainless steel. The lens body consists of two thick-wall cups made of stainless steel (6) separated by ceramic insulator (5) and strongly tightened by retaining bolts (2 in Fig. 5a) passing through the holes in thick walls of cups.

The manufacturing of lens is consists of a set of consecutive technological operations.

- There are round holes on the faces of stainless steel cups through which the thick-wall titanium cylinders (4) are inserted and the thermo-diffusion welding of titanium with stainless steel in places (13) is performed.
  - After that the stainless supply tubes (12) are attached by electron-beam welding as it shown in Fig. 3
  - Then the face surfaces of the stainless steel lens body are covered by the ceramic insulator layer (5) which surface is precisely manufactured.
  - After the two halves of the lens body are precisely assembled and strongly tightened by retaining bolts by special technology with preliminary tension of them. The inner cylindrical surface is also precisely prepared.
  - Assembled in so way lens body is heated up to several hundreds degrees and then the cold thin wall titanium cylinder (2) covered by ceramic insulator is pressed inside.
  - Electron-beam welding of the inner ( thin-wall ) and outer ( thick-wall ) titanium cylinders through round holes in stainless steel cups is then performed.
  - The final technological operation of the lens assembly is welding of cylindrical stainless details (8) with beryllium inserts (9) to the stainless steel lens body. The conical berillium inserts are first soldered into stainless cylinders and are covered by protective titanium foil. (7)
- The whole hermetic volume formed in this way and including working heated up volume  $V_h$  and buffer volumes  $V_b$  is filled with lithium under high static pressure.

Lithium is delivered to internal volume of the lens through the supplying tubes (12) passing as retaining bolts through the holes in thick walls of cups.

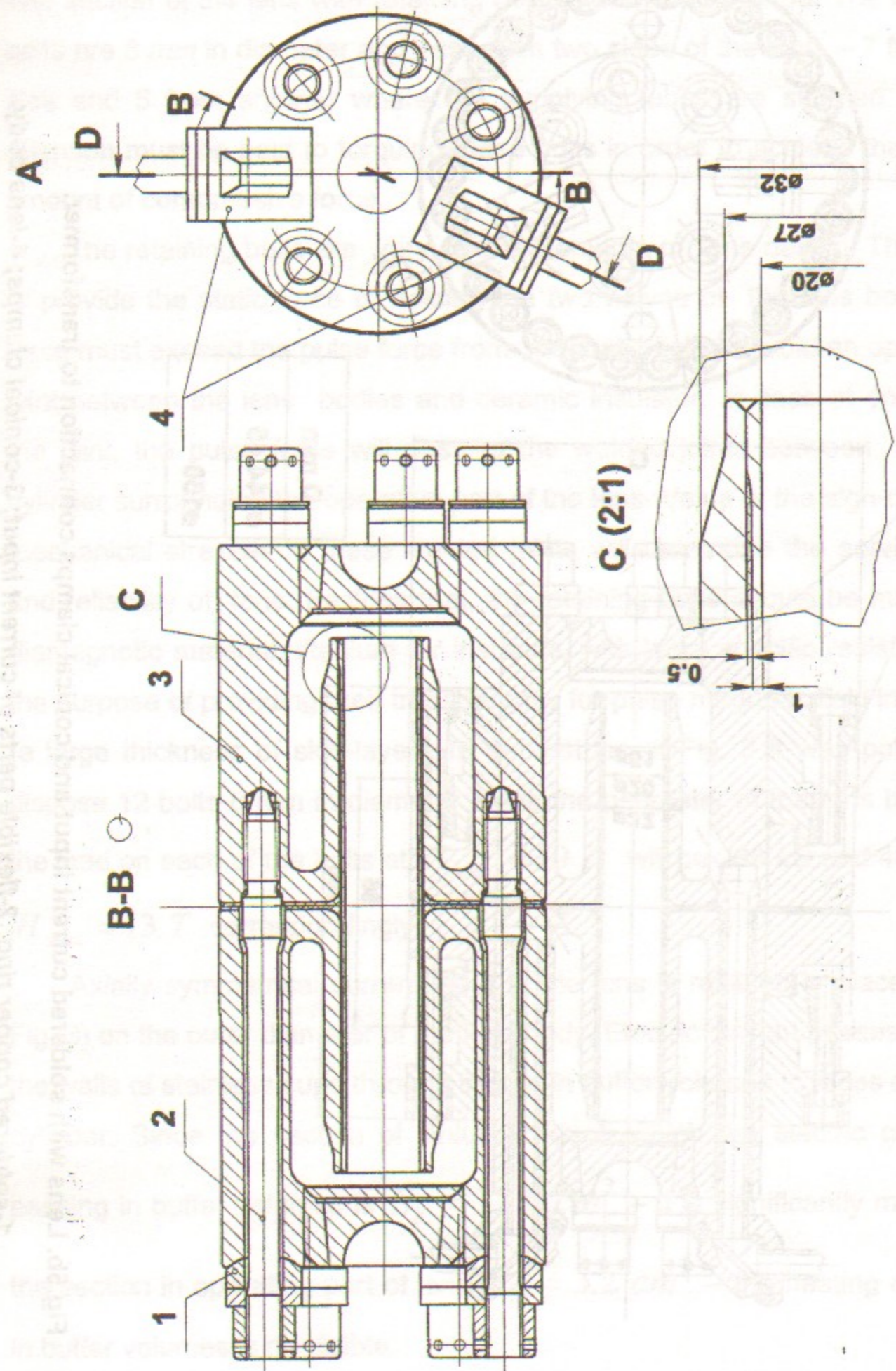


Fig.5a. Lens cross section with retaining bolts and disposition of lithium inputting tubes. 1-insulating washers; 2-retaining bolts; 3-lens body; 4-lithium inputting tubes.

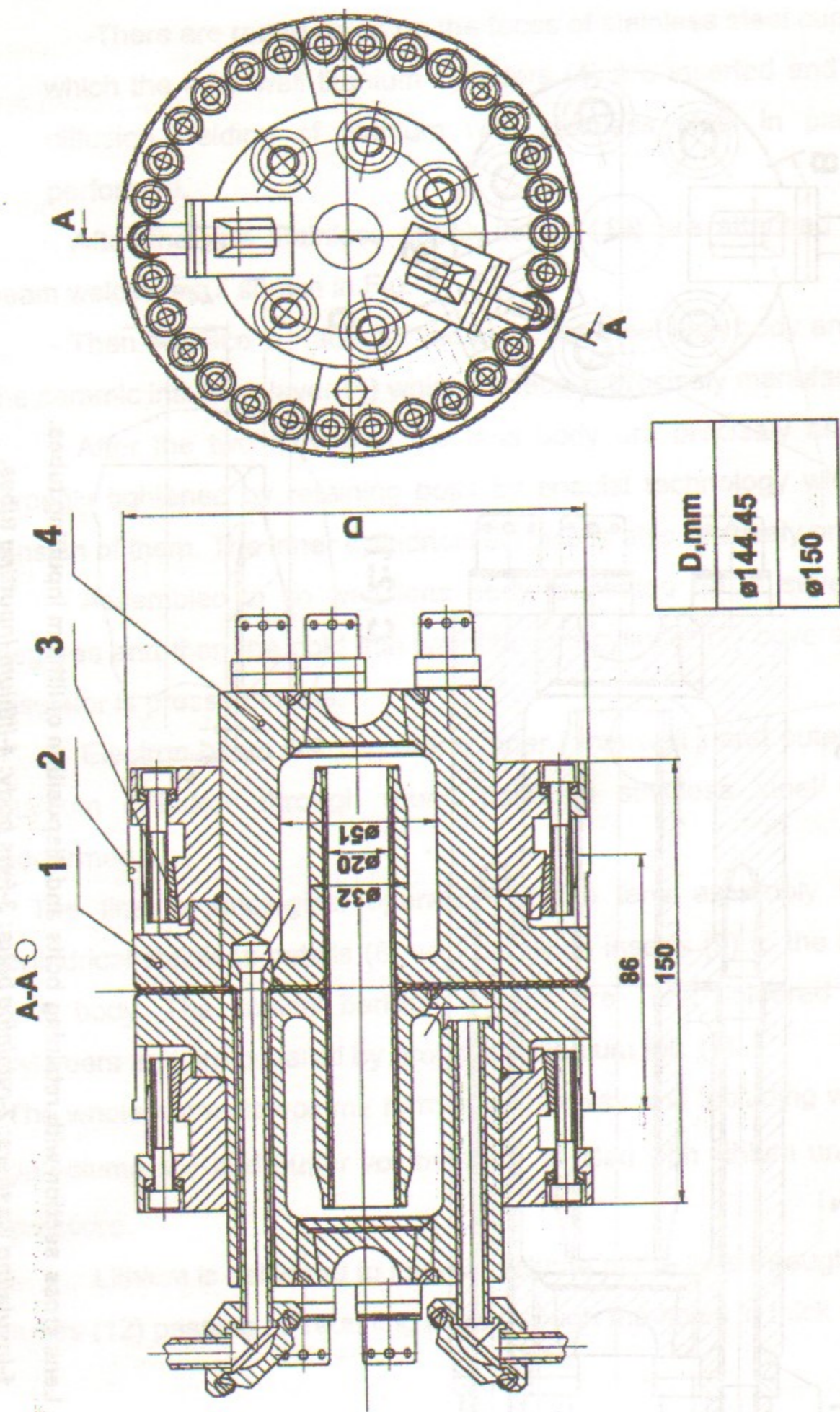


Fig.5b. Lens with soldered current input and conical clamps connection to transformer.  
 1-soldered copper ring; 2-flexible parts of current input; 3-conical clamps; 4-lens body.

The section of the lens with retaining bolts is shown in Fig. 5a. The retaining bolts are 8 mm in diameter and pass from two sides of the lens - 7 from one side and 5 from another where the supplying tubes are situated. Special attention must be paid to torquing these bolts in order to achieve the correct amount of compressive force.

The retaining bolts are very crucial elements of lens design. They have to provide the static force of holding the two halves of the lens body. This force must exceed the pulse force from magnetic field to avoid an opening of joint between the lens bodies and ceramic insulator. In case of opening of the joint, the pulse force will pass to the welded joints between two-wall cylinder surrounding the operative part of the lens. Value of the sign-changing mechanical stresses in these welded joints will determine the serviceability and reliability of lens. Besides that, the retaining bolts should be made of a diamagnetic material, titanium for instance, with large specific resistance for the purpose of providing their transparency for pulse magnetic field in the gap (a large thickness of skin-layer). In geometries of Fig. 3 it was possible to dispose 12 bolts 8 mm in diameter along the perimeter of the lens body and the load on each of the bolts at  $H_{max} = 10 T$  will be 286 kG and 483 kG at  $H_{max} = 13 T$  correspondingly.

Axially symmetrical current input to the lens is realized in places (14 in Fig. 3) on the outer diameter of the lens body. Electric current passes through the walls of stainless cups through lithium in buffer volumes to faces of lithium cylinder. Since the section of lithium through which the electric current is passing in buffer volumes is  $S_b = 12.6 cm^2$  - it is significantly more than the section in operating part of lens  $S_h = 3.2 cm^2$  - the heating of lithium in buffer volumes is negligible.

When inputting current to lens  $J > 0.5 MA$  it is necessary to pay attention to the contact transition from the secondary turn of toroidal transformer made of aluminium or copper to the lens body made of stainless steel. In contrast with lens with solid lithium which is at room temperature – in liquid lithium lens the places of contact transition will have the temperature  $\approx 200^\circ C$ . The places of current input to the lens body (14) are shown in Fig. 3. The flexible elements of the current inputs are mechanically pressed to this places. These axially symmetrical current inputs are the extensions of the secondary turn of the transformer and contact is realized on 90 mm diameter lens body. Another variant of current input is shown in Fig. 5b. The copper rings are soldered by silver to stainless lens body. These rings turn to the flexible elements of current input (2) which are pressed to the inner surface of cylindrical hole in transformer by conical clamps (3) on diameter 150 mm. In this case contact is realized on the large surface and under temperature of the transformer, cooled by water.

## 5 A SYSTEM FOR PUMPING LIQUID LITHIUM THROUGH A LENS

The task is to push out the heated-up volume of lithium from the lens immediately after the operative part of the lens has been pulse heated, with the purpose of pumping it through the heat exchanger. Geometry of the lens is depicted in Fig.3 The volume of lithium under heating  $V_h$  consists of cylindrical operating part of the lens and face transitions to current-inputting buffer volumes and is heated up to the maximum operative temperature  $T_0$ .

The current-inputting buffer volumes  $V_b$  are partially heated up to  $T_b < T_h$ .

In geometry under consideration  $V_h \approx 60 cm^3$ . It is desirable, after a pulse heating-up, to push out the volume  $V_0 > V_h \approx 100 cm^3$  to pumping system as fast as it possible. If the heated-up volume is pushed out in a time  $t = 0.5 s$  with an inter-cycle interval of 2 s ( $f=0.5 Hz$ ), the pumping system

has to provide a consumption  $R = \frac{V_0}{t} = 200 cm^3/s$ . Velocity of lithium in

different parts of closed circuit being circulated is  $u = \frac{R}{S}$  ( $S$  is the channel

section). In the cylindrical part of lens  $S_c = 3.2 cm^2$  and

$u_c = \frac{200}{3.2} = 62.5 cm/s = 0.625 m/s$ . In buffer volumes  $S_b = 3.68 cm^2$

and  $u_b = 0.54 m/s$ . The minimum flow section belongs to short ( $l = 10 cm$ ) tubes, inputting lithium to buffer volumes and going through the

lens body:  $d_p = 0.6 cm$ ,  $S_p = 0.288 cm^2$ . In them velocity of lithium is

$u_p = 6.9 m/s$ . The tubes connecting the lens with the pump have a larger

length  $l \approx 6 m$  and diameter  $d = 1 cm$ ,  $S_c = 0.8 cm^2$  and

$u = 2.5 m/s$ .

At given velocities one can calculate pressure drop at linear resistances of different parts of the circuit during pumping

$$\Delta P_i = \varepsilon \frac{\gamma}{2g} \frac{l_i}{d_{ef}} u^2$$

where  $l_i$  – the channel length,  $u$  – the liquid velocity,  $\gamma$  – its density,  $g = 9.8 \text{ m/s}^2$ ,  $d_{ef}$  – effective diameter of channel; for arbitrary section it is determined as  $d_{ef} = 4S/\Pi$ ;  $S$  – the channel section,  $\Pi$  – its perimeter;  $\varepsilon$  – the hydrodynamical resistance factor, determined by the flow regime and the hydrodynamical parameters of liquid.

For a laminar flow, when the Reynolds criterion  $Re < Re_{cr} = 2300$ ,

$$\varepsilon = \frac{A}{Re}, \text{ where } A=64 \text{ for round tubes and } A=53+96 \text{ for other sections.}$$

For a turbulent flow, when  $Re > Re_{cr}$  :  $Re = 3 \cdot 10^3 \div 10^5$

$$\varepsilon = \frac{0.32}{Re^{0.25}};$$

The Reynolds criterion  $Re = \frac{u \cdot d_{ef}}{\nu}$  depends on kinematical viscosity of liquid  $\nu$ .

Values of  $\nu$  are presented in Table 1.

	T°C	0	20	40	60	100
H <sub>2</sub> O	$\nu \frac{m^2}{s} \cdot 10^6$	1.78	1.	0.65	0.47	≈0.3
	T°C	200	300	400	600	700
Li	$\nu \frac{m^2}{s} \cdot 10^6$	1.1	0.93	0.82	0.67	0.62

In our geometry :

$$u = 7 \text{ m/s} \quad d = 0.6 \text{ cm} \quad - \quad Re = 42000 \quad \varepsilon = 0.022$$

$$u = 2.25 \text{ m/s} \quad d = 1 \text{ cm} \quad - \quad Re = 25000 \quad \varepsilon = 0.0256$$

$$u = 0.54 \text{ m/s} \quad d = 2 \text{ cm} \quad - \quad Re = 10800 \quad \varepsilon = 0.031$$

For evaluating calculations one can use the average value  $\varepsilon = 0.025$ .

So, in the circuit considered, pressure drop in its different parts make up:

$$\Delta P_i \left( \frac{kG}{cm^2} \right) = 6.25 \cdot 10^{-5} \frac{l}{d_{ef}} \cdot u^2 \left( \frac{m}{s} \right)$$

At the cylindrical part of lens :

$$l = 16 \text{ cm}, \quad d = 2 \text{ cm}, \quad u = 0.625 \text{ m/s} \quad - \quad \Delta P_1 = 2 \cdot 10^{-4} \frac{kG}{cm^2}$$

At the inputting tubes:

$$l = 2 \cdot 10 \text{ cm}, \quad d = 0.6 \text{ cm}, \quad u = 6.9 \text{ m/s} \quad - \quad \Delta P_2 = 0.1 \frac{kG}{cm^2}$$

At the connecting tubes :

$$l = 6 \text{ m}, \quad d = 1 \text{ cm}, \quad u = 2.5 \text{ m/s} \quad - \quad \Delta P_3 = 0.23 \frac{kG}{cm^2}$$

Besides this, in the circuit there will be some places with local pressure drops, namely the places with abrupt variations of section and section shape, turns, branches, and so on. There are enough such places in the circuit :

- passes from buffer volumes to the inputting tubes,
- turns of tubes at the exit from the lens,
- locking valves with complex geometry of flow sections
- branches of connecting tubes at the entry to the pump,
- entries and exits of the distributing valves of the pump.



Pressure drops in places with such local resistances are determined by formula:

$$P_i = \varepsilon_i \frac{\gamma}{2g} u^2$$

where the characteristic velocity of flow  $u$  is calculated for minimum effective cross section. In simple geometries the hydrodynamical resistance factor  $\varepsilon_i$  doesn't exceed unity –  $\varepsilon_i < 1$ . In our case:

$$\Delta P_i \left( \frac{kG}{cm^2} \right) = \varepsilon_i \cdot 2.5 \cdot 10^{-3} \cdot u^2 \left( \frac{m}{s} \right)$$

hence only the places where the velocity exceeds  $1 m/s$  are to be correctly evaluated. For example, in the places where the inputting tubes go to buffer

volumes, where  $u = 6.9 m/s$   $\varepsilon_i = 0.5$  –  $\Delta P_i \approx 0.05 \frac{kG}{cm^2}$ . In the places

where the inputting tubes leave the lens and turns by  $90^\circ$   $\varepsilon_i \approx 0.1$  and

$\Delta P_i \approx 0.01 \frac{kG}{cm^2}$ . In all other places of local nonuniformities there is a

possibility to enlarge the sections and make the velocity  $u < 1 m/s$ , so the

pressure drops will not exceed  $\Delta P_i < 0.01 \frac{kG}{cm^2}$ . Pressure drop at the pump

can be neglected since its effective cross sections are significantly larger and velocity is significantly lower than those considered earlier.

The calculation shows that with time of pumping out lithium  $\tau = 0.5 s$  in the circuit under consideration the summary pressure drops at the linear and local resistances will not exceed:

$$P_0 = \sum P_i(lin) + \sum P_i(loc) < 1 \frac{kG}{cm^2}$$

## 5.1 THE EXPERIMENTAL MEASUREMENTS OF HYDRODYNAMICAL PARAMETERS OF THE LITHIUM CIRCUIT

To get more exact information about local resistances of elements of circuit with complex geometry of sections measurements of pressure drops using water instead of lithium were undertaken. These experiments were carried out on specially made prototypes of lithium circuit elements. Water at room temperature has kinematical viscosity practically equal to lithium at temperature interval  $200 \div 250^\circ C$  (Table 1). So, water can be used for very simple experiments. Water was pumped through the model of investigated element with real geometry of flow section. Pressure at the inlet of element was measured by height of water column in the vertically placed glass tube. Free discharge to vessel with definite volume  $V$  was at the outlet of element, and velocity of liquid  $u$  was defined by measuring of water expenditure  $W = V/t$  and  $u = W/S$  where  $S$  is the flow section of inputting tube,  $t$  – time of the vessel filling.

The objects for measurements were:

**Geometry 1.** Smooth bending of tubes with  $180^\circ$  and  $90^\circ$  turn and radius  $40 mm$ . It imitates connecting tubes from lens, situated in transformer, to locking valves. (See Fig. 5 a,b)

**Geometry 2** Sharp turn of the tubes with 90° angle at the outlet of lens.  
(See Fig. 3)

**Geometry 3** Connection of supplying tubes with buffer volumes in lens. (See Fig. 3)

**Geometry 4** Locking valves ( See Fig. 19a)

The pressure drops  $P_i(loc)$ , atm. in described geometries for different velocities are given in Table. 2

Table 2

Geometry	velocity $u$ , m/s				
	0.5	1	1.5	2	2.5
1		0.008	0.02	0.03	
2		0.005	0.018	0.025	
3		0.01	0.02	0.05	
4		0.03	0.05	0.11	0.19
$P_{\Sigma}$		0.05	0.15	0.3	0.6

Since the pressure drop is proportional to density of liquid -  $\gamma$ , for lithium with the same velocity the values of  $\sum P_i(loc)$  will be two times less than for water.

## 5.2 HYDRODYNAMIC MODEL OF THE LITHIUM CIRCUIT

For measurements of full hydrodynamical resistances of the whole lithium circuit a full-scale model including lens prototype with exact geometry of internal volumes where lithium should flow was made. Also two locking

valves and two supplying tubes each 2.3 m in length with corresponding smooth bends were manufactured (see Fig. 6-8). The pressure drop on circuit  $P_{\Sigma}$  for different water velocities in connecting tubes 1 cm of inner diameter are given in Table 2. The pressure was measured by the same method described above.

This hydrodynamical model of circuit was used also for pumping of liquid gallium-indium alloy by electromagnetic pump. Work of locking valves and methods of measurements of liquid metal velocity by magnetic flowmeter were investigated, also. It will be described below.

As the next step we have planned to carry out the same testing with liquid lithium. From this model the next investigations will be fulfilled:

- development of methods of measurement of liquid lithium velocity by flow-meter and temperature distribution by thermocouples,
- development of methods of automatic management of the process of heating, melting and freezing of lithium and static pressure control,
- long time running of the system

## 6 LIQUID LITHIUM PUMPS

It was shown in experiments with hydrodynamical model that if the pump provides pressure  $\Delta P = 0.5 atm$  (including pressure drops on pump and heat exchanger) then the velocity of lithium in connecting tubes with flow section  $S_t = 0.8 cm^2$  will be  $u_t = 2.5 m/s$ . Velocity of lithium in working

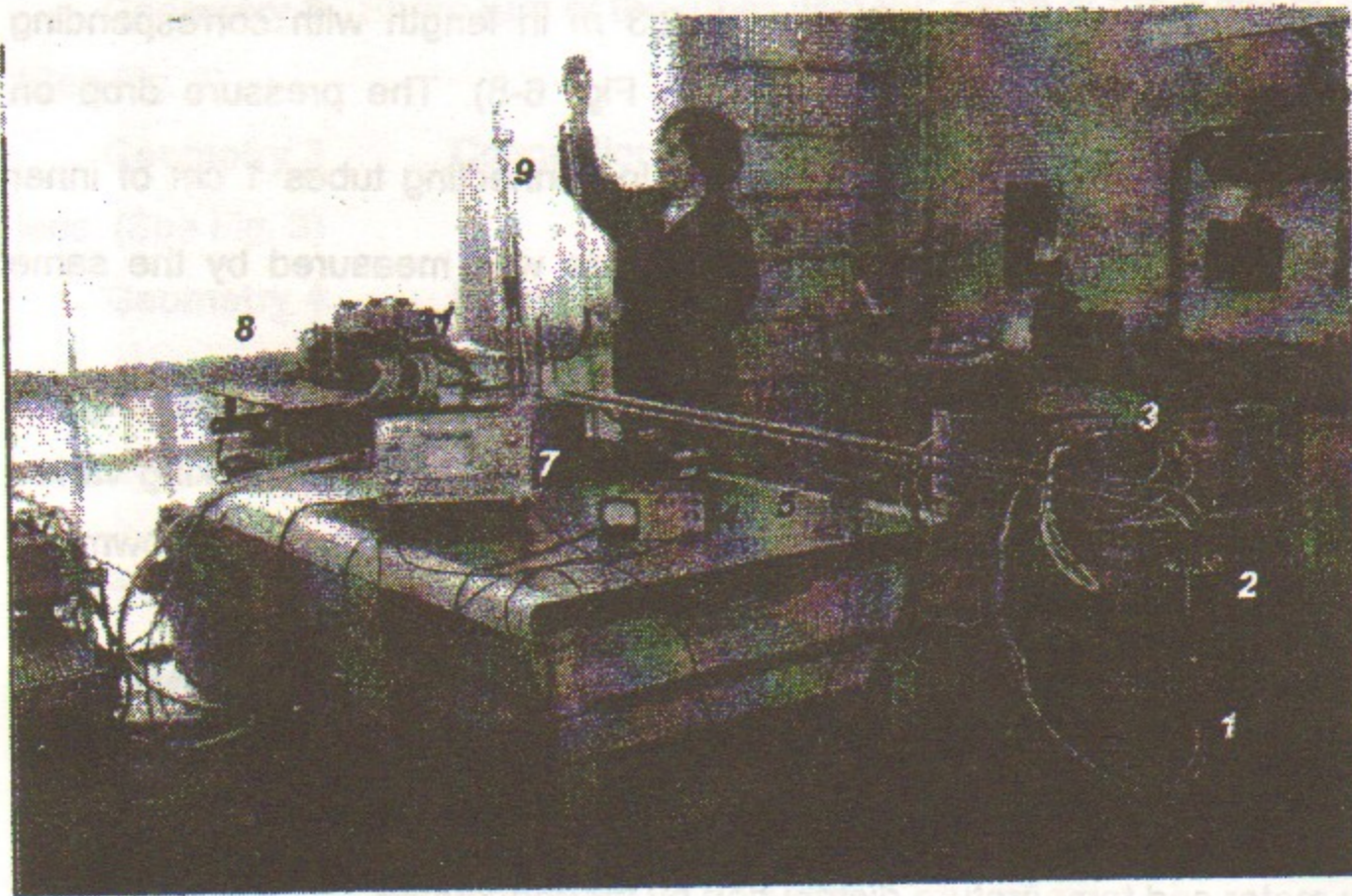


Fig. 6.



Fig. 7.

- 1 - dummy lens;
- 2 - locking valves;
- 3 - valves power supply;
- 4 - flowmeter gauge;
- 5 - flowmeter;
- 6 - heat exchanger;
- 7 - spiral tupe pump;
- 8 - pump power supply;
- 9 - gallium vessel and glass tube for pump pressure measurements.

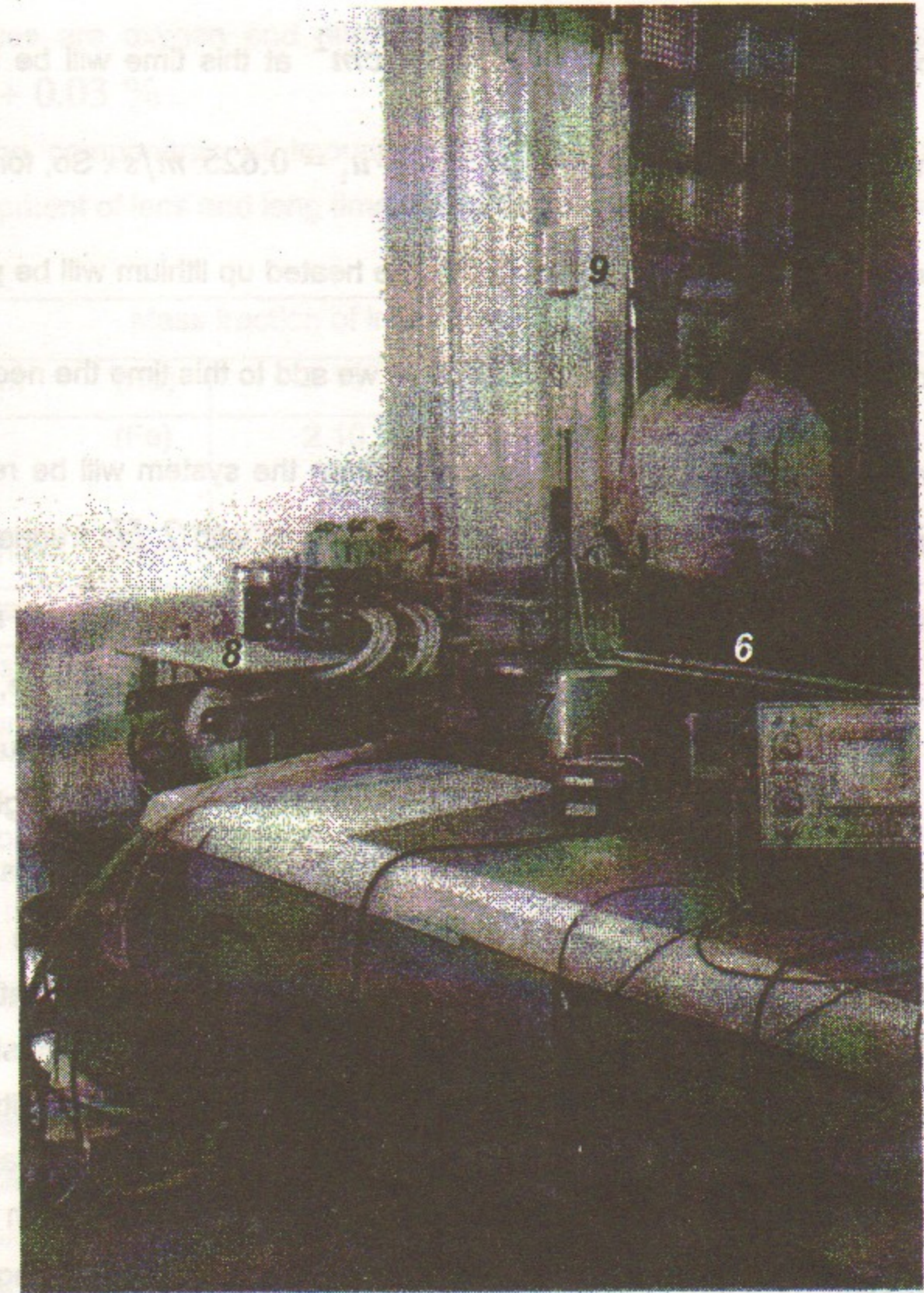


Fig. 8.  
6 - heat exchanger; 7 - spiral type pump;  
8 - pump power supply; 9 - gallium vessel and glass tube for pump pressure measurements.

part of lens with cross-section  $S_l = 3.2 \text{ cm}^2$  at this time will be so, for length of working part of the lens  $u_l = \frac{S_t}{S_l} \cdot u_t = 0.625 \text{ m/s}$ . So, for length of working part of the lens  $l_l = 15 \text{ cm}$  the heated up lithium will be pushed out from lens by time  $t = \frac{l}{u_l} = 0.24 \text{ s}$ . If we add to this time the necessary time reserve for locking valves operation, then the system will be ready to the next cycle through  $t \approx 0.5 \text{ s}$ , so it can operate with  $2 \text{ Hz}$  frequency.

It means that for proposed frequency  $0.6 \text{ Hz}$  we have a good reserve and demands to pump pressure are not so extreme, thus  $P = 0.5 \div 1 \text{ atm}$ . When we choose the type and design of pump the more complex demands appear from the necessity to provide high static pressure  $P_{st} \approx 300 \text{ atm}$  in the system. The additional demand is a high corrosion resistance of elements of lithium circuit in liquid lithium to provide reliable work during several years. These demands can be satisfied at first by correct choice of material for lithium circuit. It's known that the most stable materials in liquid lithium are tungsten, molybdenum, pure iron and its alloys with refractory metals (tungsten, molybdenum, niobium, vanadium) and also special kinds of stainless steel with minimal nickel content, titanium and its alloys, some sorts of ceramics, for example berillium oxide  $BeO$ , magnesium oxide  $MgO$  or ceramic materials based on berillium nitrides  $BeN$ ,  $Be_2N_3$ . Corrosion rates of these materials quickly rises with temperature. The speed of this process is defined, at first, by purity of lithium. The most dangerous

impurities are oxygen and nitrogen and their content should not exceed  $0.02 \div 0.03 \%$ .

The components of impurities in lithium which will be used during development of lens and long time testing are performed below (See Table3)

Table 3

Mass fraction of impurities, %, not more than:				
Sodium (Na)		$3 \cdot 10^{-3}$	Magnesium (Mg)	$2 \cdot 10^{-3}$
Iron (Fe)		$2 \cdot 10^{-3}$	Silicon oxide (SiO)	$6.4 \cdot 10^{-3}$
Aluminium (Al)		$2 \cdot 10^{-3}$	Manganese (Mn)	$3 \cdot 10^{-4}$
Nitrogen (N)		$3 \cdot 10^{-3}$	Lead (Pb)	$1 \cdot 10^{-3}$
Potassium (K)		$3 \cdot 10^{-3}$	Tin (Sn)	$1 \cdot 10^{-3}$
Calcium (Ca)		$6.9 \cdot 10^{-3}$	Barium (Ba)	$5 \cdot 10^{-3}$

For work in radiation conditions it is necessary to use lithium isotope  ${}^7\text{Li}$ . It has tritium production cross-section three orders of magnitude less than the  ${}^6\text{Li}$  one. Natural lithium consists of 92.6% of  ${}^6\text{Li}$  and 7.4% of  ${}^7\text{Li}$ .

Besides that, the corrosion rate strongly depends on state of lithium contacting with material surface. The corrosion rate is minimal if lithium is motionless and it increases with lithium velocity growth near the surface of material. Also corrosion rate increases if friction between elements of construction wetted by lithium is appeared. Therefore it's necessary to avoid quickly moving parts in lithium system such as bearings and quickly spinning details. But more dangerous is the electrocorrosion. It is caused by electric

current in contact regions between metal surface and liquid lithium in liquid lithium electromagnetic pump.

These circumstances, especially necessity of high static pressure have not allowed us to choose any of industrial pumps and it defined our choice of type and design of pump for this aim. Two types of pump were considered in this project.

1. The electromechanical pump of piston type, working in cyclic mode with frequency about 1 Hz.

2. The electromagnetic pump of spiral type and continuous operation.

## 6.1 PISTON TYPE PUMP

Design of this pump is shown in Fig. 9 a,b. It is a thick-wall cylinder made of ferromagnetic steel (4 in Fig. 9a). The cylinder is closed by two face disks (1) welded rigidly to cylinder, so the hermetic volume is realized and it can sustain the necessary static pressure. Face disks turns into two cylindrical magnetic poles and there is ferromagnetic insert of plunger (6) between poles moving from one pole to another by force of magnetic field. The plunger (5) consists of two nonmagnetic pipes ( of stainless steel or titanium ) connected with ferromagnetic insert. The narrow gap between plunger surface and internal surface of cylinder is  $d \approx 0.1 \text{ mm}$ . It provides a minimum friction between them. With such gap and enough length of plunger lithium flow in this gap will be negligible, as it will be shown below. To decrease corrosion of material in places of friction between plunger and cylinder (at the ends of plunger) the surface of plunger is covered by thin

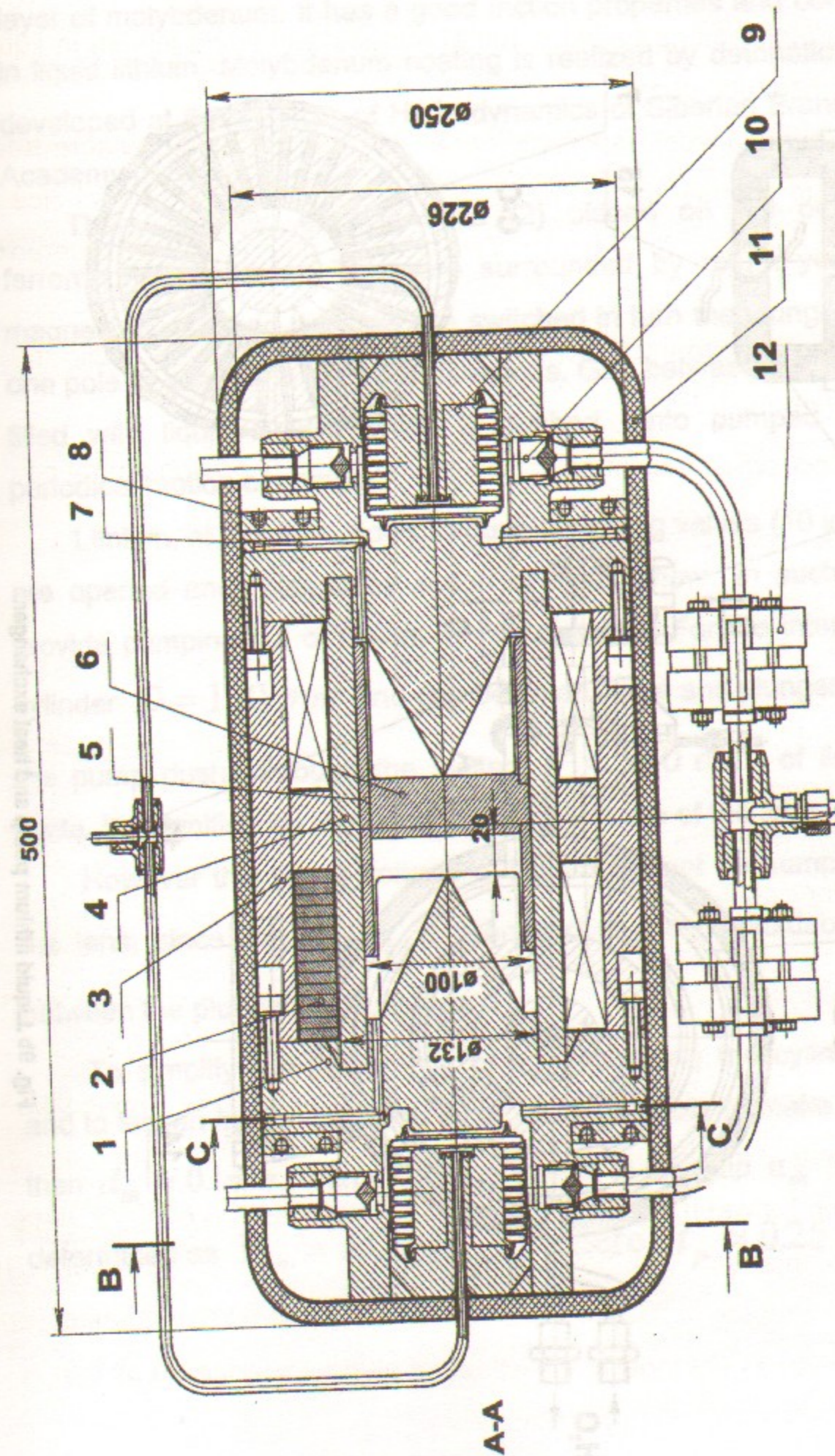


Fig.9a. Liquid lithium pump and heat exchanger.  
 1-face disks; 2-exciting coil; 3-return yoke; 4-inside ferromagnetic wall of cylinder; 5-plunger;  
 6-ferromagnetic insert of plunger; 7-cooling channels of heat exchanger; 8-cooling water;  
 9-system to apply and control of liquid lithium static pressure; 10- switching valves;  
 11 - thermo-insulation; 12 -system to measure liquid flow rate; 13-joint of liquid lithium pipes;  
 14 -pump support; 15 -contacts for potential measurements.

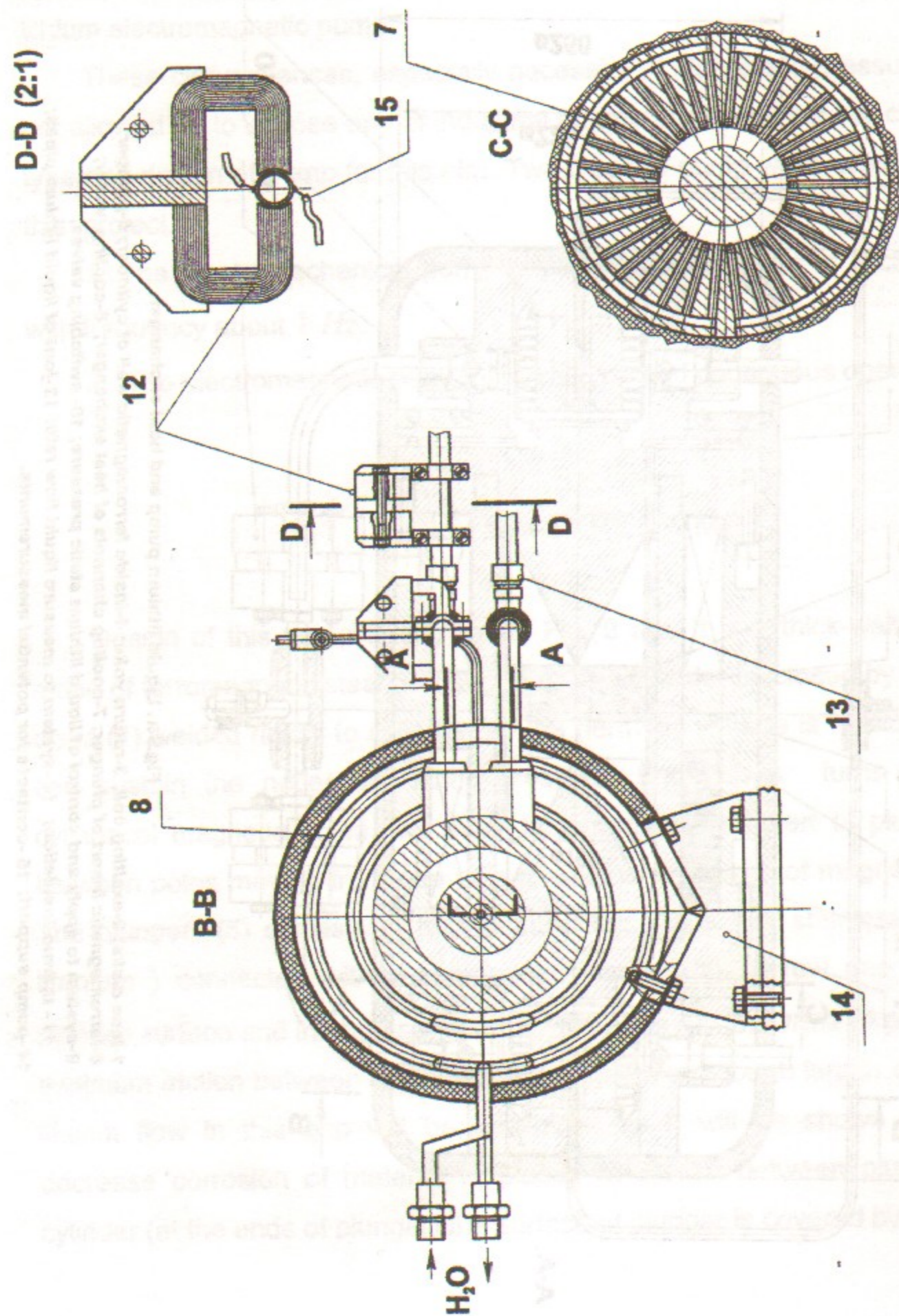


Fig. 9b. Liquid lithium pump and heat exchanger.

layer of molybdenum. It has a good friction properties and corrosion stability in liquid lithium. Molybdenum coating is realized by detonation-gas method, developed at the Institute of Hydrodynamics of Siberian Branch of Russian Academy of Sciences.

There are two exciting coils (2) placed on the outer surface of ferromagnetic cylinder. They are surrounded by return yoke (3), closing magnetic flux. When the coils are switched in turn the plunger moves from one pole to another in opposite directions. Gap between poles and plunger is filled with liquid lithium which is pushed into pumped system during periodical motion of plunger.

Lithium, at this time, flows through switching valves (10 in Fig. 9a) which are opened and closed by action of lithium flow in such succession to provide pumping out of lithium in one direction. For the internal diameter of cylinder  $D = 100 \text{ mm}$  and gap between poles and plunger  $h = 20 \text{ mm}$ , the pump pushes through the system  $V = 160 \text{ cm}^3$  of liquid lithium per cycle. It's significantly more than working volume of the lens.

However this whole volume of lithium will not be pumped only through the lens, since its part  $V_{sh}$  is branched to the unavoidable shunting gap between the plunger and cylinder  $d_{sh}$ .

To simplify the technology of manufacturing the cylinder and plunger and to lessen friction between them, it is desirable to make the gap not less than  $d_{sh} \approx 0.1 \text{ mm}$ . With velocity of lithium in this gap  $u_{sh}$  the value  $V_{sh}$  is determined as  $V_{sh} = \pi D d_{sh} u_{sh} t_p$  where  $t_p \approx 0.25 \text{ s}$  - time of pump

operation . Since it is desirable that  $V_{sh}$  is significantly lower than  $V_p$  , e.x.

$V_{sh} < 0.1V_p = 15cm^3$  , velocity of lithium is to be  $u_{Li} \leq 2 m/s$  . With a very

narrow and long gap, its effective hydrodynamical value  $d_{ef} = \frac{4S}{\Pi}$  will equal

$d_{ef} = 2d_{sh}$  and the Reynolds criterion  $Re = \frac{u_{sh} \cdot d_{ef}}{\nu}$  is

$Re = 400 \ll Re_{cr}$  . It means that flow will be a pure laminar one. With

this, the value of hydrodynamical resistance factor  $\varepsilon = \frac{57 \div 93}{Re}$  may be

taken to be  $\varepsilon \approx \frac{80}{Re} = \frac{80 \cdot \nu}{u_{sh} \cdot d_{ef}}$  . Then a pressure drop at this gap with the

length  $l$  will be

$$\Delta P = \varepsilon \frac{l}{d_{ef}} \frac{\gamma}{2g} u_{sh}^2 = \frac{80\nu}{d_{ef}} \left( \frac{l}{d_{ef}} \right) \frac{\gamma}{2g} u_{sh}$$

that is in linear dependence on velocity. The pressure drop at the gap equals the pressure of pump  $\Delta P = P_0$  , so an "egress" of lithium to the shunting gap

$V_{sh} = \pi D d_{sh} u_{sh} t_p$  is determined as  $V_{sh} = \frac{P_0 g d_{sh}^2 \pi D t_p}{20 \nu \gamma (l/d_{ef})}$  and with

$p_0 = 0.5 kG/cm^2$  ,  $l = 200 mm$  ,  $d_{sh} = 0.1 mm$  ,  $t_p = 0.25 s$  will equal  $V_{sh} = 3 cm^3$  . In reality this value will be slightly larger because of

unavoidable "egress" in distributing valves of the pump. Its value depends on design and manufacturing technology of valves.

The coils of pump will be wound with oxidized aluminium wire to obtain thermal stability. These coils will be used also for heating of pump to the melting point of lithium.

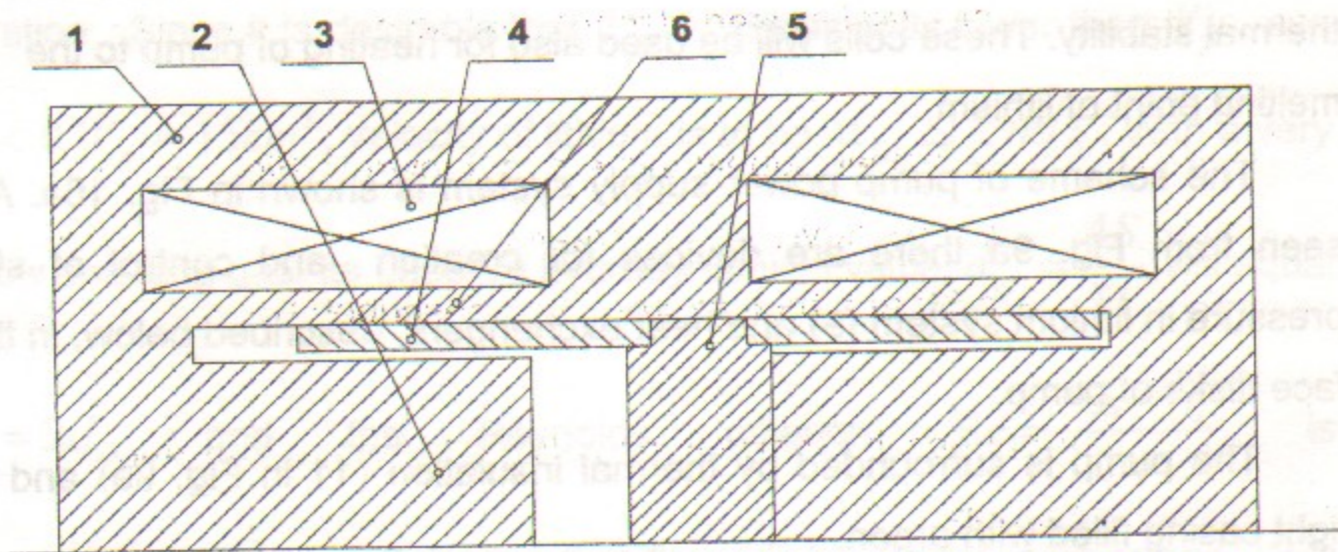
The scheme of pump power supply system is shown in Fig. 16a. As it seen from Fig. 9a there are devices for creation and control of static pressure in lithium system (9) and heat exchangers, described below, in thick face disks of pump.

The pump is surrounded by thermal insulation (11 in Fig. 9a) and air-tight casing filled with argon.

## MAGNETIC SYSTEM OF LIQUID LITHIUM PUMP.

Magnetic system of pump ( Fig. 10 ) consists of cylindrical shape yoke (1) with poles (2) and two exciting coils (3) supplied in turn. Space between poles and coils forms a cylinder (6) in which plunger (4) is situated. The plunger consists of two diamagnetic pipes (4) (of stainless steel or titanium ) connected by means of ferromagnetic insert (5). Two exciting coils, switched in turn, force the plunger to move periodically between poles.

The peculiarity of this magnetic system is, that coils are separated from the internal part of pump by means of thick-wall ferromagnetic cylinder which partly closes magnetic flux. Field value between poles is not affected by this ferromagnetic layer practically, only value of magnetic field induction in return yoke is increased. ( Fig. 13,14 ) The thick-wall ferromagnetic cylinder is very responsible element of the whole construction because it works under high static pressure conditions ( up to  $300 kG/cm^2$  ) in liquid lithium. So it must be made of *homogeneous material*. If it is made of nonmagnetic



1-return yoke; 2-poles of yoke; 3-exciting coils; 4-plunger;  
5-ferromagnetic insert of plunger; 6-ferromagnetic wall of cylinder.

Fig.10. Magnetic system of liquid lithium pumping unit.

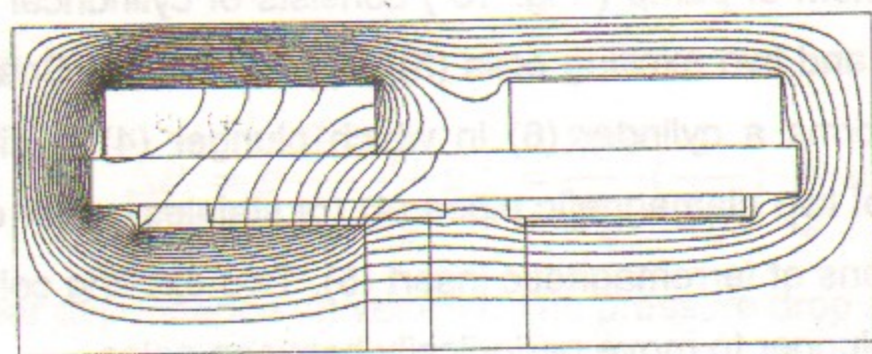


Fig.11. Flux lines. Diamagnetic wall.

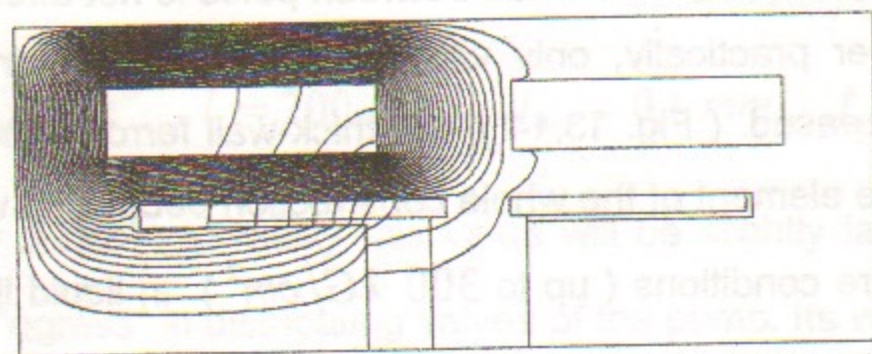


Fig.12. Flux lines. Ferromagnetic wall.

-1*1	-4*5	-3*6	-3*4	-2*5	-1*4	-1*5	-1*5	-1*5	-1*3
*98	x053	x085	x232	*404	*48	x000	-x00	x002	x001
*68	x264	x331	x492	1*45	*001	-x01	-x00	x004	x004
*28	.400	.516	.641	1.24	.075	.004	.008	.008	-.00
*926	.245	.274	.425	1.32	.059	-.01	-.01	-.01	-.01
3*08	.170	.014	.249	2.28	1*94	.029	.028	.028	2*79
3*38	9*36	8*25	6*88	3.45	2*81	3*79	3*75	3*96	2*74
2*73	8*12	8*12	6*36	3.11	3*01	3*47	3*61	3*45	2*31
2*26	7*39	7*91	6*12	3.08	3*09	3*37	3*47	3*16	2*11
2*08	6*97	7*78	5*81	3.06	3*10	3*32	3*39	3*04	2*04

Fig. 13. Digit map of  $B_x$ . Diamagnetic wall.  $I=5$  kA.

-9*0	-14*	-14*	-13*	-12*	-2*8	*54	*46	*46	*44
-5*0	-14*	-14*	-13*	-11*	-2*9	*22	*46	*46	*00
*91	-x00	x128	x141	*173	-1*2	x001	-x00	x001	x000
*389	x136	x344	x373	1*27	*669	-x00	-x00	x002	-x00
2*29	20*5	20*6	21*4	23*1	3*65	*15	*336	*337	*424
6*18	20*5	20*5	21*2	23*0	6*74	*899	*346	*337	*270
7*54	*748	.114	.120	2.14	*007	.00	-.00	*789	*794
7*46	12*5	.114	9*11	3.88	2*02	*583	*731	*754	*504
6*83	11*7	11*1	8*52	3.10	1*94	*858	*750	*754	*504
6*20	11*4	11*0	8*17	2.97	2*08	1*02	*773	*703	*481
5*28	11*2	10*9	7*93	2.94	2*17	1*09	*790	*694	*475

Fig. 14. Digit map of  $B_x$ . Ferromagnetic wall.  $I=5$  kA.

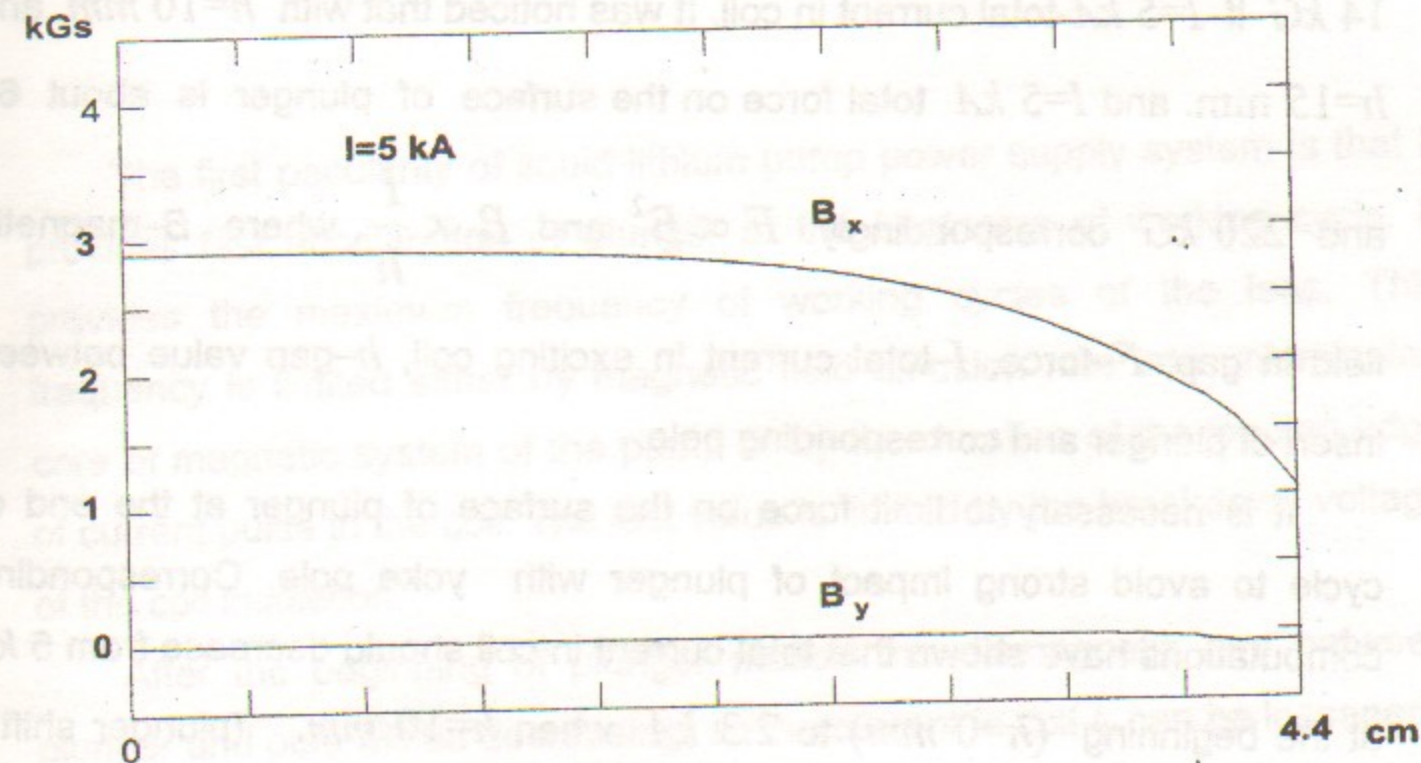


Fig.15.  $B_x$ ,  $B_y$  on the surface of plunger.



substance ( stainless steel or titanium ) then a radial gap between body of yoke and insert of plunger appears. It causes appearance of additional resistance in magnetic circuit and results in branching of magnetic flux to symmetrical part of yoke ( Fig. 11,12 ).

For field calculations in this geometry a special computer code MERMAID developed at BINP was used. This program was used also to choose the geometry of pump earlier.

Main attention during computations was given to ensure sufficient force on the surface of plunger at the initial position and to avoid iron saturation in yoke. This calculations were made for three positions of plunger :  $h=0, 10, 15 \text{ mm}$ . – shift from initial position. Results for  $h=0 \text{ mm}$  are performed at Fig. 14,15 where the digit map of  $B_x$  and field components  $B_x, B_y$  behaviour along the surface of the plunger are shown. Based on data obtained total force on the surface of plunger was estimated. At the initial position it is about  $14 \text{ kG}$  if  $I=5 \text{ kA}$ -total current in coil. It was noticed that with  $h=10 \text{ mm}$ . and  $h=15 \text{ mm}$ . and  $I=5 \text{ kA}$  total force on the surface of plunger is about 60

and  $220 \text{ kG}$  correspondingly.  $F \propto B^2$  and  $B \propto \frac{I}{h}$ , where  $B$ -magnetic

field in gap,  $F$ -force,  $I$ -total current in exciting coil,  $h$ -gap value between insert of plunger and corresponding pole.

It is necessary to limit force on the surface of plunger at the end of cycle to avoid strong impact of plunger with yoke pole. Corresponding computations have shown that total current in coil should decrease from  $5 \text{ kA}$  at the beginning ( $h=0 \text{ mm}$ ) to  $2.3 \text{ kA}$  when  $h=10 \text{ mm}$ . (plunger shift) and to  $1.1 \text{ kA}$  when  $h=15 \text{ mm}$ . and force acting on the plunger will not exceed  $15 \text{ kG}$ . To avoid impact it is possible to switch off the coil a little

earlier time. These considerations together with mechanical parameters of pump and duration of working cycle define the parameters of coils power supply system.

This calculations of values and distribution of magnetic field in gap and induction in core is valid only for stationary case or laminated core. Really, only the cylindrical poles and return yoke are laminated. When current is switched in exciting coils quickly – in cylinder, endcaps and in lithium itself eddy currents will be induced. They will prevent from field diffusion into magnetic gap. Therefore the magnetic system of pump is characterized by the electrical time constant of relaxation to stationary state. The plunger dynamics and the maximum frequency of working cycles is determined by this constant. Value of time-constant will be defined experimentally in real construction during its manufacturing.

## THE POWER SUPPLY SYSTEM OF LIQUID LITHIUM PUMP.

The first peculiarity of liquid lithium pump power supply system is that it provides fast acceleration of plunger at the beginning of working cycle. It provides the maximum frequency of working cycles of the lens. This frequency is limited either by magnetic field diffusion rate into unlaminated core of magnetic system of the pump or by the duration of the leading edge of current pulse in the coil. The last value is limited by the breakdown voltage of the coil insulation.

After the beginning of plunger motion the diamagnetic gap between plunger and pole will be decreasing, so the current in coil  $I_L$  can be lessened.

The second peculiarity of power supply system is possibility to stop the plunger at the end of working motion to avoid impact with pole of magnetic core.

For calculation of parameters of coils and elements of circuit the following conditions will be taken into account: to create  $H = 0.3 T$  magnetic field the current  $5 kA \cdot turns$  is necessary. Let us set the maximum current in coil  $I_{max} = 20 A$  and maximum voltage on it  $U_{max} = 100 V$ . Then the number of turns in coil will be defined as

$$w = \frac{5 \cdot 10^3 A \cdot turn}{20 A} = 250 turns.$$

Trivial estimation of parameters of magnetic system gives the following values:

$$L_M = 3 \cdot 10^{-2} H$$

$$R_M = 0.75 Ohm$$

Fig. 16a shows the scheme of power supply system. Structurally the generator consists of two transistor switches with special circuits for dissipation of stored energy. At the initial moment the capacitors  $C_1$  and  $C_3$  are charging up to voltage  $E_0$ , the transistors  $V_1$  and  $V_2$  are closed. Upon switching on the transistor  $V_1$ , the  $C_1$  discharges to the magnet's coil

$L_M R_M$ . In this case the leading edge of a current pulse with the time duration

$$\tau = \pi \cdot \sqrt{L_M \cdot C_1}$$

is formed. After discharging of capacitor  $C_1$  to voltage

$$E_0 R_M / (R_M + R_1) \text{ the current in coil will be } I = \frac{E_0}{R_1 + R_M}$$

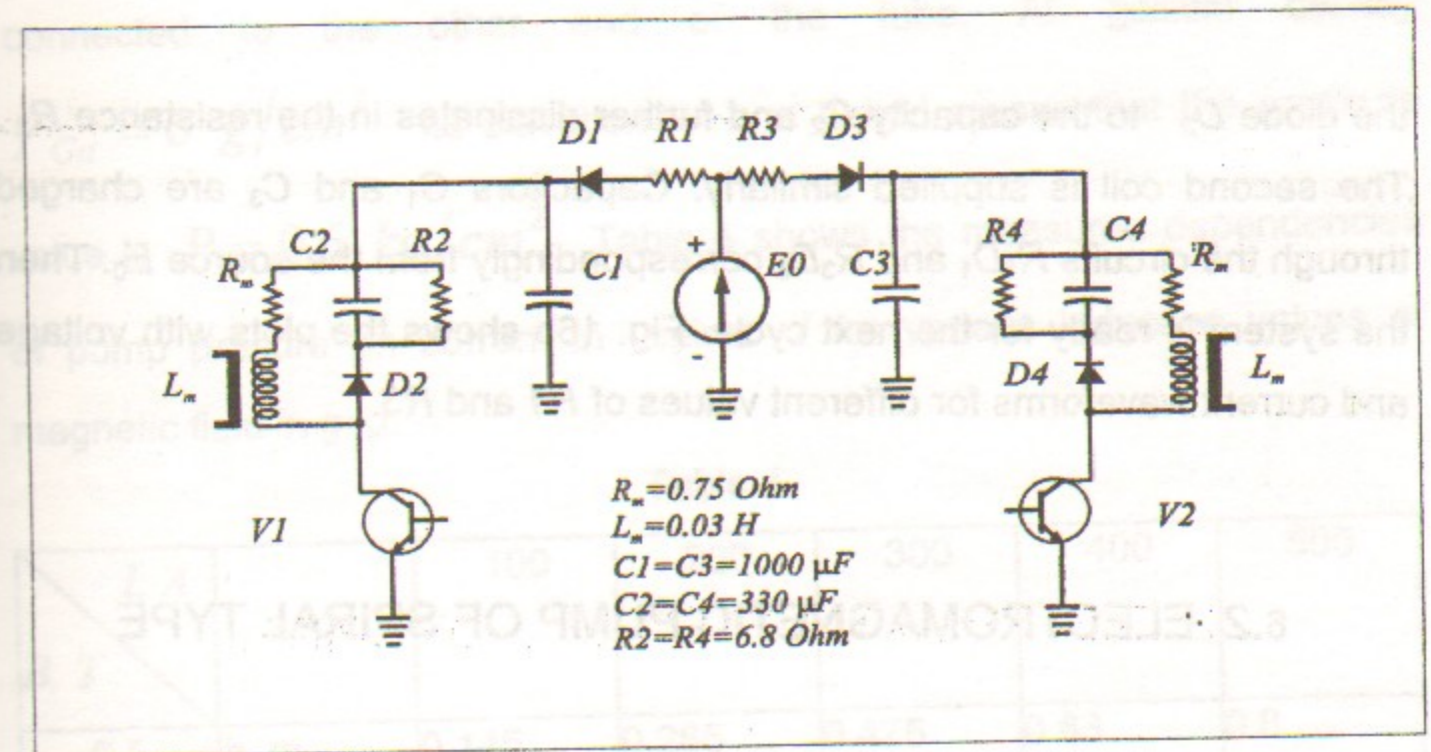


Fig. 16a

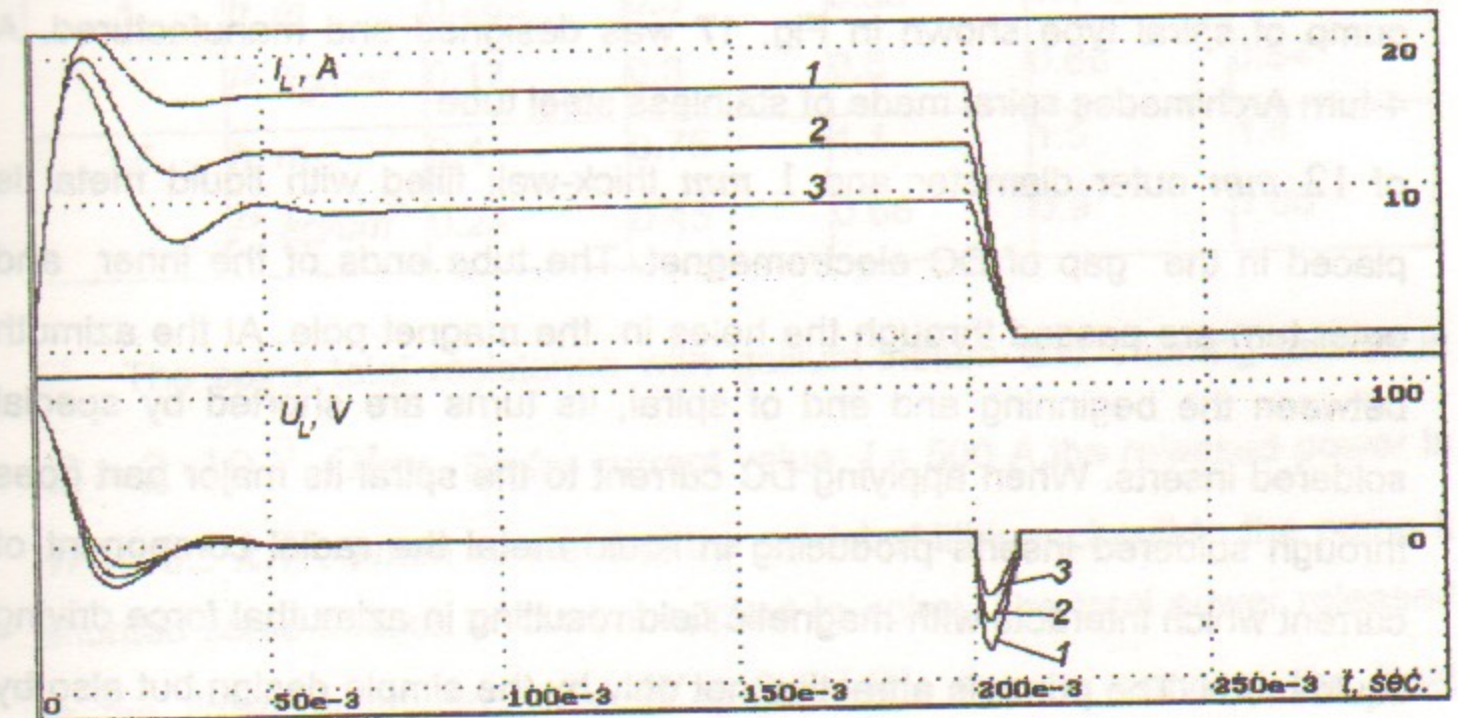


Fig. 16b.  $R_1=R_3=4.5 Ohm(1); R_1=R_3=6.8 Ohm(2); R_1=R_3=10 Ohm(3)$ .

and the top of pulse is formed. We can change current by changing of  $R_1$ . The pulse trailing edge is generated during the switching off of the transistor  $V_1$ . In this case the stored energy from magnet's coil is transmitted through

the diode  $D_2$  to the capacity  $C_2$  and further dissipates in the resistance  $R_2$ . The second coil is supplied similarly. Capacitors  $C_1$  and  $C_3$  are charged through the circuits  $R_1D_1$  and  $R_3D_3$  correspondingly from the source  $E_0$ . Then the system is ready for the next cycle. Fig. 16b shows the plots with voltage and current waveforms for different values of  $R1$  and  $R3$ .

## 6.2 ELECTROMAGNETIC PUMP OF SPIRAL TYPE

For carrying out experiments with the gallium-indium alloy on the hydrodynamic model of lithium circuit described above the electromagnetic pump of spiral type shown in Fig. 17 was designed and manufactured. A 4-turn Archimedes spiral made of stainless steel tube of 12 mm outer diameter and 1 mm thick-wall filled with liquid metal is placed in the gap of DC electromagnet. The tube ends of the inner and outer turn are passed through the holes in the magnet pole. At the azimuth between the beginning and end of spiral, its turns are shorted by special soldered inserts. When applying DC current to the spiral its major part goes through soldered inserts producing in liquid metal the radial component of current which interacts with magnetic field resulting in azimuthal force driving liquid metal. The pump is attracting not only by the simple design but also by that the spiral can be made of the tube with cross section the same as that used for connecting tubes of the lithium circuit withstanding the same static pressure.

The pressure produced by the pump is measured by the height of liquid metal column in vertical tube. The vessel with gallium-indium alloy is connected to one end of the tube and a 2.5 m long vertical glass tube is

connected to the other end of the tube. At gallium density  $\gamma_{Ga} = 6 \text{ g/cm}^3$  its elevation to 1 m height means that the pressure value is  $P = 0.6 \text{ kg/cm}^2$ . Table 4 shows the measured dependencies of pump pressure on current in spiral  $I$  for various induction values of magnetic field in gap.

Table 4.

$I, A$		100	200	300	400	500
0.5	$h, m$	0.145	0.265	0.475	0.63	0.8
	$P, \text{ kg/cm}^2$	0.09	0.16	0.285	0.38	0.48
1	$h, m$	0.285	0.5	0.83	1.1	1.4
	$P, \text{ kg/cm}^2$	0.17	0.3	0.5	0.66	0.84
1.5	$h, m$	0.4	0.75	1.1	1.5	1.8
	$P, \text{ kg/cm}^2$	0.24	0.45	0.66	0.9	1.08

The spiral total resistance with gallium-indium and shorting inserts is  $R = 2 \cdot 10^{-3} \text{ Ohm}$ . So for current value  $I = 500 \text{ A}$  the released power is  $W = 0.5 \text{ kW}$ . When connecting the model of lithium circuit to the pump it shunted some fraction of current applied to spiral. The total power released in the liquid metal circuit is  $W = 0.6 \text{ kW}$ . For its removal the heat exchanger is placed on one of feeding tubes. The heat exchanger made of 0.2 mm thick thin-wall tube of 20 mm in diameter and 1 m in length made of stainless steel is coaxially placed on the connecting tube and tightened on its ends. Water flows between tubes producing thus the heat exchanger with heat removal area of  $360 \text{ cm}^2$ .

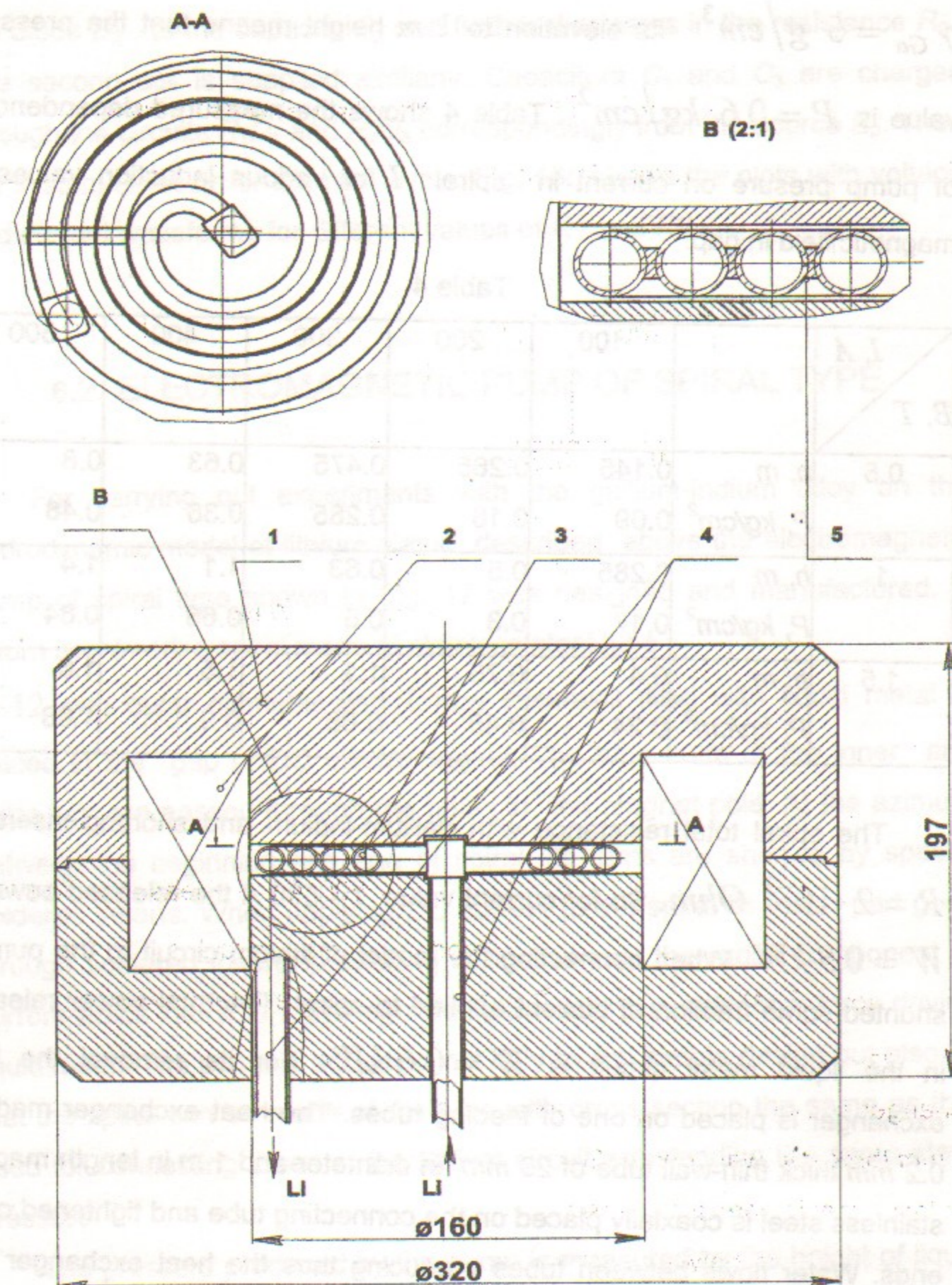


Fig.17. Liquid lithium pump of spiral type.

1-DC magnet yoke; 2-exciting coils; 3-spiral tube; 4-liquid lithium inputs;  
5-soldered shortening inserts.

The stand with the pump and liquid metal circuit is given in Fig. 6-8. In a feeding tube with the cross section of  $0.8 \text{ cm}^2$  the pump produced the velocity of the gallium-indium alloy of  $u = 2 \text{ m/s}$  in the closed circuit at the field value of  $1.5 \text{ T}$  and current of  $500 \text{ A}$ . It means that under the same

conditions, in liquid lithium the velocity of  $u_{Li} = \sqrt{\frac{\gamma_{Ga}}{\gamma_{Li}}} \cdot u_{Ga} \cong 3.46 u_{Ga}$

can be achieved.

At present, some modifications of the spiral pump are considered to minimize the corrosion effects. Such a pump could be promising alternative for the piston type electromechanical pump.

## 7 LITHIUM CIRCUIT COOLING

As shown in Section 4, with the optimum choice of the pulse duration corresponding to the ratio  $\delta/r = 0.7$  the mean temperature of the active lithium volume does not depend on either the lens diameter or the lithium specific resistance, which is constant and determined only by magnetic field value on the surface. At  $H=100 \text{ kOe}$  the pulse heating value  $T=60^\circ$ . If the

energy released in lens per pulse is  $Q = Tc\gamma\pi R^2 l$  the power is  $W = Qf$ , where  $c$  – is the lithium heat capacity,  $\gamma$  – its density,  $f$  – cycle frequency. In the geometry under consideration at  $f = 1 \text{ Hz}$ ,  $W = 6 \text{ kW}$ .

Taking into account the additional heat generated in the lens buffer volumes,

surving as current input, the total power generated in lithium can be estimated as  $W \approx 10 \text{ kW}$ . If the heat exchanger surface for heat removal is more than  $300 \text{ cm}^2$ , the heat flow through the cooled surface will be  $q \leq 30 \text{ W/cm}^2$  quite moderate for water cooling. The problem is complicated by the fact that the heat has to be removed from the surface heated up to the temperature  $T \approx 200^\circ \text{C}$ . For this aim, the water pressure in water cooling circuit is assumed to be  $P = 15 \text{ atm}$  at which the water boiling temperature increases up to  $T \approx 200^\circ \text{C}$ . The circulation of water in such closed circuit is provided by the standard commercially available pump and the pressure is produced and controlled by the same equipment used for producing the static pressure in the lithium circuit. Cooling the closed water circuit of higher pressure is made by conventional technical water.

The design of heat exchangers located on the ends of the piston pump is given in Fig. 9 a,b.

There are two heat exchangers in the system, so each of them is to absorb a power  $Q \approx 5 \text{ kW}$ . The power is absorbed when the liquid lithium flows through the radial channels drilled in the iron face disks of pump (7 in Fig. 9 a,b). Number of channels is 30. Diameter of channel is  $d_c = 0.5 \text{ cm}$ , distance to the face surface is  $d_{Fe} = 0.5 \text{ cm}$ . The heat exchange is performed practically with whole cover surface  $S \approx 230 \text{ cm}^2$  in area, so the heat flow equals  $q = \frac{Q}{S} = 22 \frac{\text{W}}{\text{cm}^2}$ . The temperature drop between the channel surface and those of cover is as follows:

$$\Delta T_{Fe} \approx \frac{q d_{ef}}{\lambda_{Fe}}, \text{ where } \lambda_{Fe} = 0.6 \frac{\text{W}}{\text{cm} \cdot \text{degree}} - \text{the thermal conductivity of}$$

iron at  $T=250^\circ \text{C}$ ,  $\Delta T_{Fe} \approx 20 \text{ degree}$ . The temperature drop between

lithium and channel wall takes the following form:  $\Delta T_{W-liq} = \frac{q}{\alpha}$ , where  $\alpha$  is

the heat transfer factor, determined by hydrodynamical regime of flow of

liquid and its thermophysical properties:  $\alpha = \frac{Nu \cdot \lambda_{Li}}{d_c}$ , where  $Nu$  is the

Nusselt number,  $\lambda_{Li}$  - the thermal conductivity of lithium,

$\lambda_{Li} = 0.45 \frac{\text{W}}{\text{cm} \cdot \text{degree}}$  at  $T=250^\circ \text{C}$ . If  $P$ , complete consumption of

lithium in the system, equals  $P = 200 \text{ cm}^3/\text{s}$  through each of the channels

will go  $P_1 = \frac{200}{30} = 6.7 \text{ cm}^3/\text{s}$  and velocity will be

$u_{Li} = \frac{P_1}{S_c} = \frac{6.7}{0.2} = 33.3 \text{ cm}^3/\text{s}$ . With such velocity, the flow of lithium in the

channel will be a laminar one since the Reynolds criterion

$Re = \frac{u_{Li} \cdot d_c}{\nu} = 1665 < Re_{cr} = 2300$ . Here  $\nu$  is the kinematical viscosity

factor of lithium. At  $T=250^\circ \text{C}$   $\nu \approx 10^{-6} \text{ cm}^2/\text{s}$ . For a laminar flow

$Nu \approx 5$ , so  $\alpha = \frac{5 \cdot 0.45}{0.5} = 4.5 \frac{\text{W}}{\text{cm}^2 \cdot \text{degree}}$  and

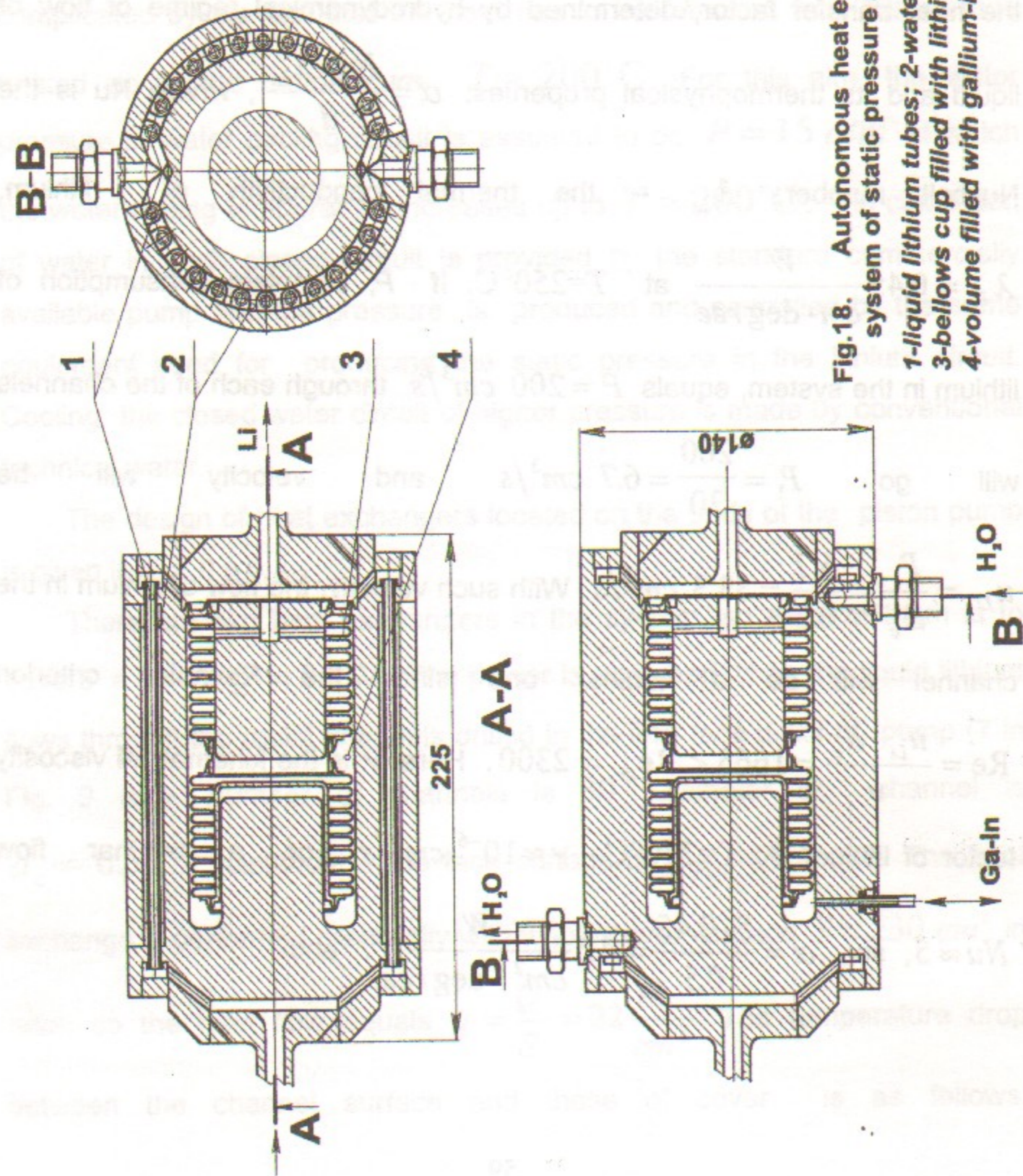


Fig.18. Autonomous heat exchanger with system of static pressure adjustment.  
 1-liquid lithium tubes; 2-water cooling channels;  
 3-bellows cup filled with lithium;  
 4-volume filled with gallium-indium alloy.

$$\Delta T_{W-liq} = \frac{22}{4.5} = 4.9 \text{ degree} .$$

At the pump cover there are brazed-to copper disks, cooled by water.

In case of development of some alternate version of the pump in the process of further work, for example an electromagnetic pump of spiral type, the heat exchanger could be an autonomous device. The design of such heat exchanger combined with the device producing the static pressure in the lithium circuit is given in Fig. 18.

## 8 LOCKING VALVES

First experimernents with liquid lithium lens of large diameter described in [9] have shown that pulsed heating of lithium in working part of lens results in appearance of compression wave spreading along the whole lithium circuit. Such percussive loads on elements of liquid lithium circuit will cause lowering of reliability of its work during many millions cycles. This problem was solved by means of installation of locking electromagnetic valves at the inlet and outlet of lens. These valves are quickly locked and unlocked on small time interval during which the current pulse will pass through lithium. It is necessary to mention that valves should only damp the compression wave, not to close the lithium flow completely during lens work. Valves should have a little leakage to provide a fast restoration of initial presure distribution after damping the percussive load from thermal expansion of lithium. It allows to open valves quickly and provides liquid lithium circulation. Such leakage may be realized by superficial thread on the sealing surface of

piston. For the project under discussion locking valves were developed and their design is shown in Fig. 19a

The locking valve is a thick-wall ferromagnetic cylinder with light free moving ferromagnetic piston having some azimuthal slits for liquid lithium passage when its inlet hole is open.

The valve has two exciting coils. Switching on one coil creates magnetic field attracting the piston in position where it covers the inlet hole. Switching on the other coil causes opening of valve. The longitudinal shift of piston can be adjusted from 2 to 4 mm.

The pattern of flux lines when different coils are switched separately and the digit map of longitudinal component of field  $B_x$  for  $I=3$  kA are shown in Fig. 19 b,c. When  $I=3$  kA force acting on the piston is about 1 kG when maximum shift is 3 mm.

Coils are wound on the aluminium body isolated by oxide layer. The coils contain 100 turns and are made of oxidized aluminium wire. It provides radiation and thermal resistance of coils.

The system of power supply provides fast  $\approx 10$  ms switching on of current up to 30 A in coil closing the valve and also fast switching on of current in the other coil through time interval  $\tau$ . Value of  $\tau$  can be changed between 0.1-0.5 s. Testing has shown that a weight 1 kg was elevated by piston agreeing with the computation.

The speed of valve operation is the most important parameter. Investigations of the valve operation speed were carried out on hydrodynamical model of lithium circuit using liquid gallium-indium alloy instead of liquid lithium. (see Fig. 6,7) The oscillograms of signal from gallium-indium flow-meter are shown in Fig. 20.

Because of complex geometry of valve flow section the pressure drop on it was measured experimentally using water ( see chapter 5). The results of

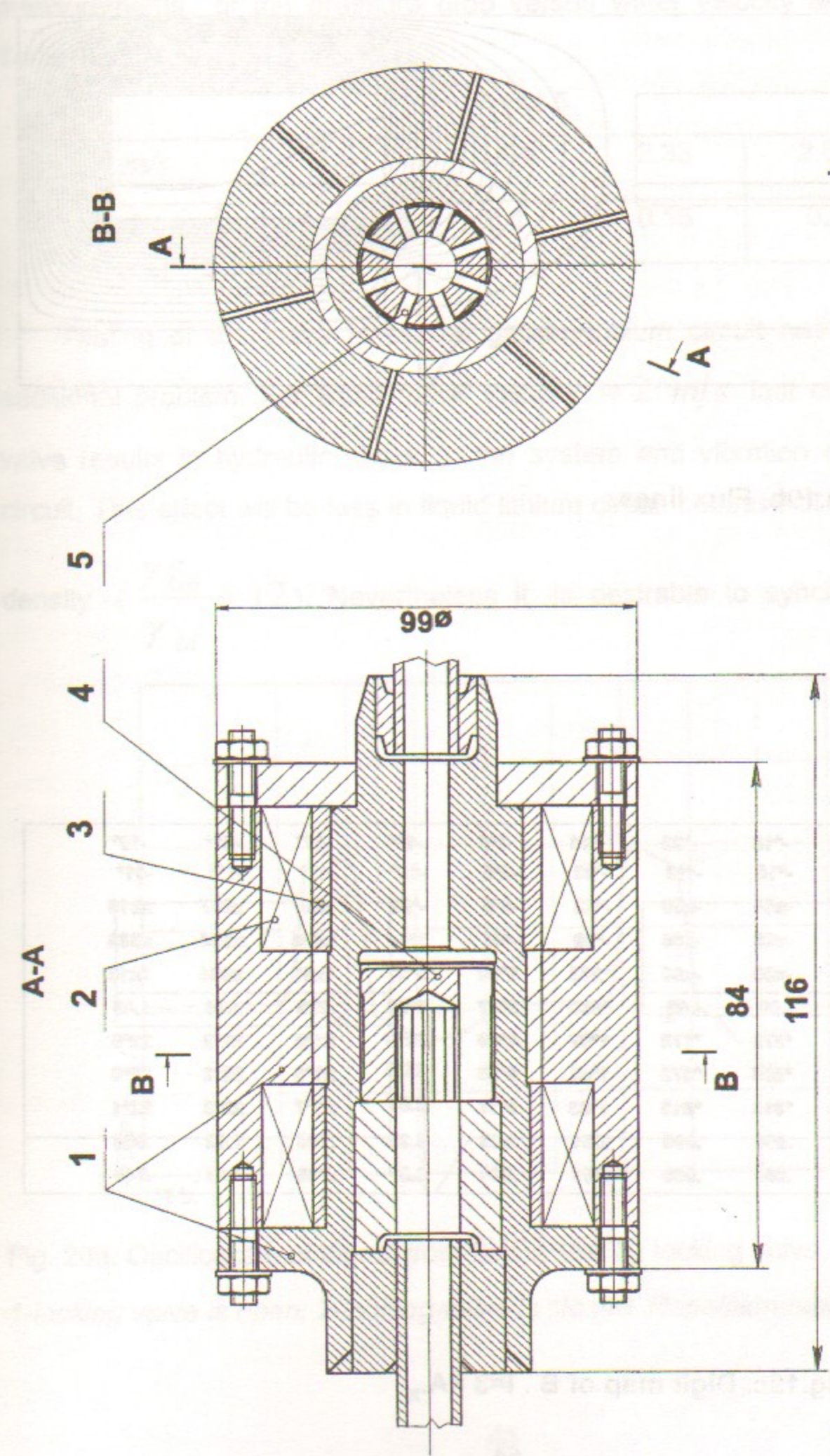


Fig. 19a. Locking valve.

1-ferromagnetic yoke of valve; 2- exciting coil; 3-diamagnetic supporting tubes; 4-plunger; 5-slits for lithium flow.

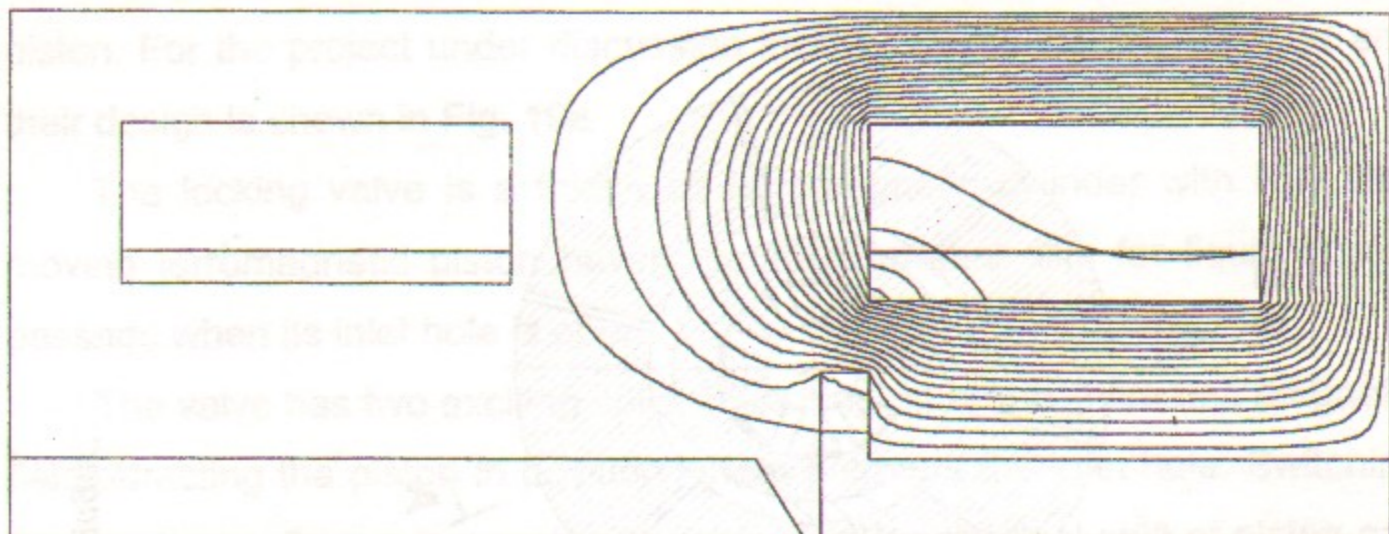


Fig.19b. Flux lines.

*00	*15	*16	*23	*98	-3*5	-10*	-11*	-11*	-10*
*07	*16	*16	*13	*68	-2*6	-10*	-11*	-11*	-11*
*04	-x00	-x00	-x00	*42	-1*8	*98	x047	x027	x016
*00	-x00	-x00	-x00	*00	-*58	*714	x824	x504	x553
*021	-x00	-x00	-x00	*283	1*00	2*37	1x10	x834	1x10
*067	-00	-00	-00	*690	2*87	6*33	.973	.994	1.48
*145	*304	*279	*178	1*07	4*89	22*6	21*6	22*2	22*0
*135	*282	*295	*379	1*41	5*50	25*6	21*8	22*2	22*0
*122	*267	*316	*813	1*83	5*17	5.67	21*7	22*3	22*1
.000	.000	.000	.000	.001	.003	1.32	.706	1.02	.880
.000	.000	.000	.000	.001	.004	3.07	.789	.995	.745

Fig.19c. Digit map of B . I=3 kA.<sub>x</sub>

measurements of the pressure drop versus water velocity are shown in Table 5.

Table 5

$u, m/s$	1.54	1.94	2.33	2.54
$P, kg/cm^2$	0.052	0.1	0.15	0.2

Testing of the valve in closed gallium-indium circuit has shown one additional problem. For liquid metal velocity  $\approx 2 m/s$  fast closing of the valve results in hydraulic shock in the system and vibration of the whole circuit. This effect will be less in liquid lithium circuit because of lower lithium density ( $\frac{\gamma_{Ga}}{\gamma_{Li}} \approx 12$ ). Nevertheless it is desirable to synchronize the



Fig. 20a. Oscillogram of signal from flow-meter by locking valve operation 1-locking valve is open; 2-locking valve is closed. Repetition rate 0.2 Hz.



working cycles of piston type pump, with the working cycles of lens to switch the valve on when lithium velocity is zero.

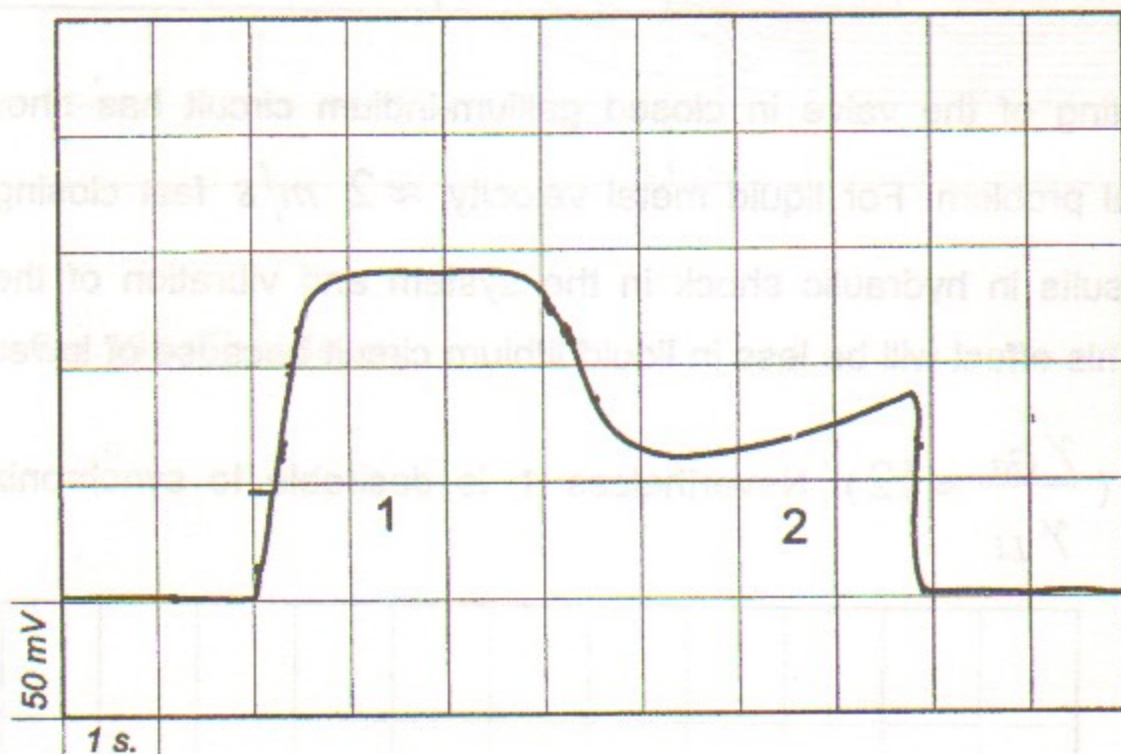


Fig. 20b. Oscillogram of signal by flow-meter calibration.

1-time of flowing out of gallium indium from vessel;

2 time of flowing out of gallium indium from connecting tube.-

## 9 MEASURES AND ADJUSTMENT OF STATIC PRESSURE IN LITHIUM SYSTEM.

Lithium has a big coefficient of volume thermal expansion  $\alpha = 1.8 \cdot 10^{-4} \text{ deg}^{-1}$  and its volume increases on  $1.5 \cdot 10^{-2}$  after melting. When we heat up and melt lithium and create a high static pressure

in it, variation of lithium volume can be more than 5%. So with full lithium volume about  $1000 \text{ cm}^3$  the changing part of volume can be  $\Delta V \cong 50 \text{ cm}^3$ . For compensation of such variations there is a special device for volume changing, adjustment and measurements of static pressure in liquid lithium. (position 9 in Fig. 9a) It is the elastic cup made of bellows with disk welded on the end. The solid cylinder is inserted into cup and the bellows compression is limited by the end of this cylinder. The bellows is inserted into a rigid cylindrical casing. Tension of bellows is limited by the bottom of casing. Compression and tension of bellows corresponds to necessary variations of lithium volume. Internal volume of bellows is connected with lithium system and filled with liquid lithium. Volume between bellows and cylindrical casing is filled with oil or gallium-indium alloy and connected with thick-wall cylinder by means of thin and long tube. The thick-wall cylinder is placed under room temperature and there is a piston with ordinary rubber seal in it. Pressure in this cylinder is equal to pressure in liquid lithium and is measured by usual manometer. The piston is being moved by electric motor which provides the automatic adjustment and stabilization of pressure in lithium system.

## 10 LIQUID LITHIUM FLOW-METER

The construction of magnetic flow-meter is based on interaction between moving conductor and magnetic field. The magnetic core with cylindrical gap between poles is put on the tube with flowing liquid metal. (position 12 in Fig. 9b)

Constant magnetic field in gap is created by cobalt-samarium magnet inserted into break of yoke. Field in gap is  $\approx 0.3 T$ . There are contacts (15 in Fig 9b) on the opposite sides of tube on diameter perpendicular to magnetic field for measuring of rising potential difference. Estimations have shown that for lithium velocity  $u = 1 m/s$  the induced potential difference should be  $E \approx 1 mV$ . The calibration of flow-meter was done with gallium-indium alloy. Measurements of time of flowing out of definite volume of liquid metal through the tube with flow-meter gives the velocity of liquid metal through the known section of the tube. Velocity of liquid metal was adjusting by changing of levels of inlet and outlet ends of tube.

Oscillogram of signal from flow-meter by flowing out of gallium-indium from vessel (9 in Fig.6-8) is shown in Fig.20b.

## 11. LAYOUT OF LITHIUM SYSTEM IN ANTIPROTON TARGET STATION

The lens is placed inside the toroidal transformer and it is connected to its secondary coil by the conic clamps providing reliable contact at current over  $0.5 MA$ . The transformer is suspended to the lower part of the transformer module of size  $220 \times 80 \times 40 cm$  being the component of radiation protection and together with the unit it is lowered down to the proton beam axis Fig.21 a,b. On the neighbouring units the target and other units of the target station are located. The components of the lithium circuit should not surpass a longitudinal size of  $40 cm$ . In the selected version on the lens design, tubes

for supplying liquid lithium go out from one side of the lens and turn immediately to the plane perpendicular to the beam axis as shown in Fig.21 a,b. In this case, they protrude beyond the transformer no more than  $20 mm$ . Then tubes make one more turn and connect to the locking valves placed in a free space to the left of the transformer. Such a complicated geometry of connecting tubes is necessary to reduce the system lens-transformer longitudinal size to its minimum. The system of remote disconnection of lithium circuit (Fig. 21c) is placed over the locking valve. The remotely disconnected systems transform into the long tubes connecting parts of the lithium system in the radiation zone with the pump placed over the module. These tubes pass through the holes in the removable rectangular insert mounted into the module. Since lithium connecting tubes are connected to two halves of the lens being at different potentials, they should be insulated from each other. The locking valves and the device of remote disconnection of lithium circuit are fixed strongly to the rigid bracket fixed on the transformer. In this case, they should also be isolated from each other and from the support bracket since they are connected with tubes at different potentials. Thus, both branches of lithium circuit are insulated from each other and shorted only at the point of its connection to the pump. This circuit shunts the lens. However it has very high inductance compared to that of the lens so the value of the branched current can be neglected.

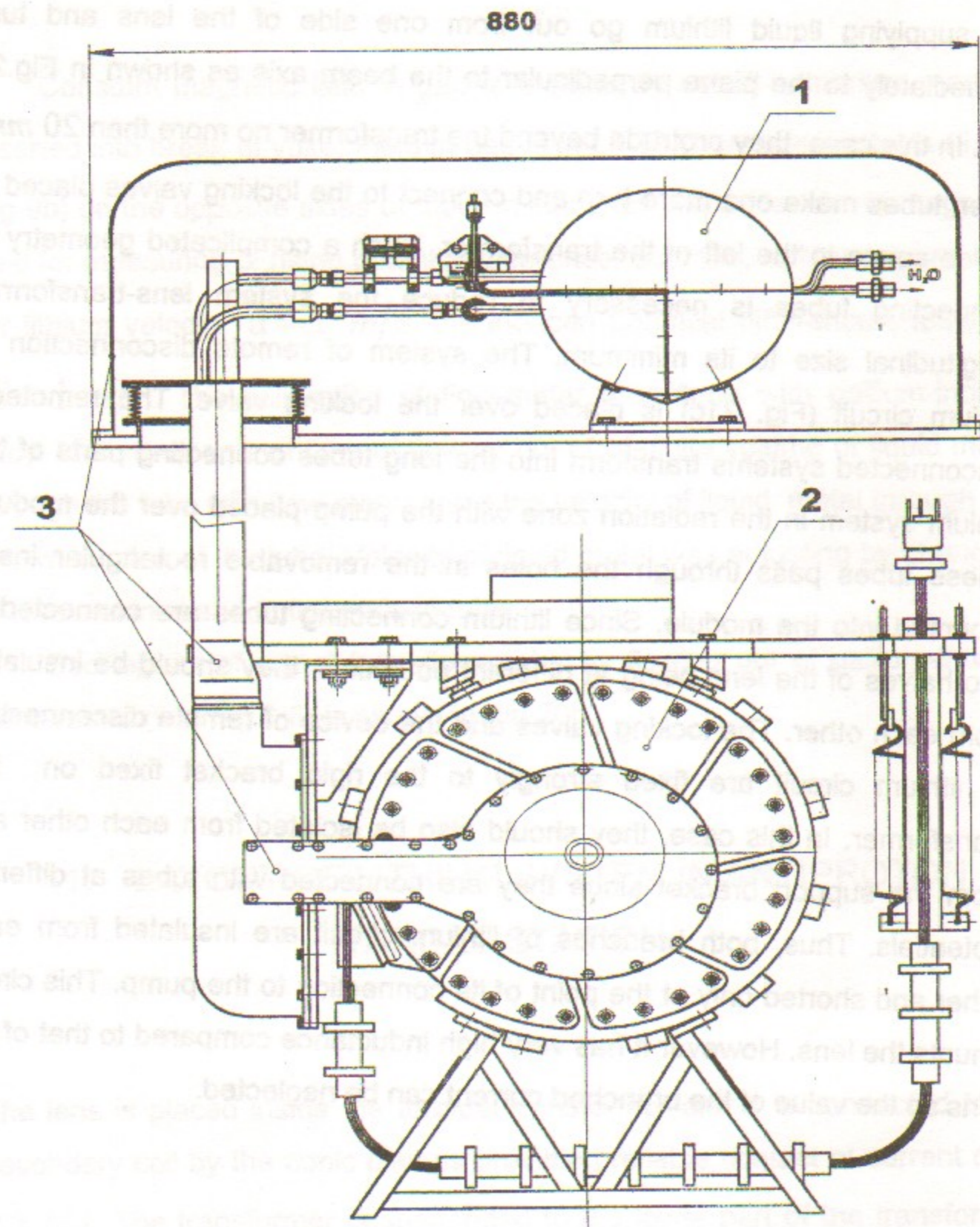


Fig. 21a. Layout of the system in antiproton target station.  
 1-liquid lithium pump; 2-toroidal transformer; 3-lithium circuit protection.

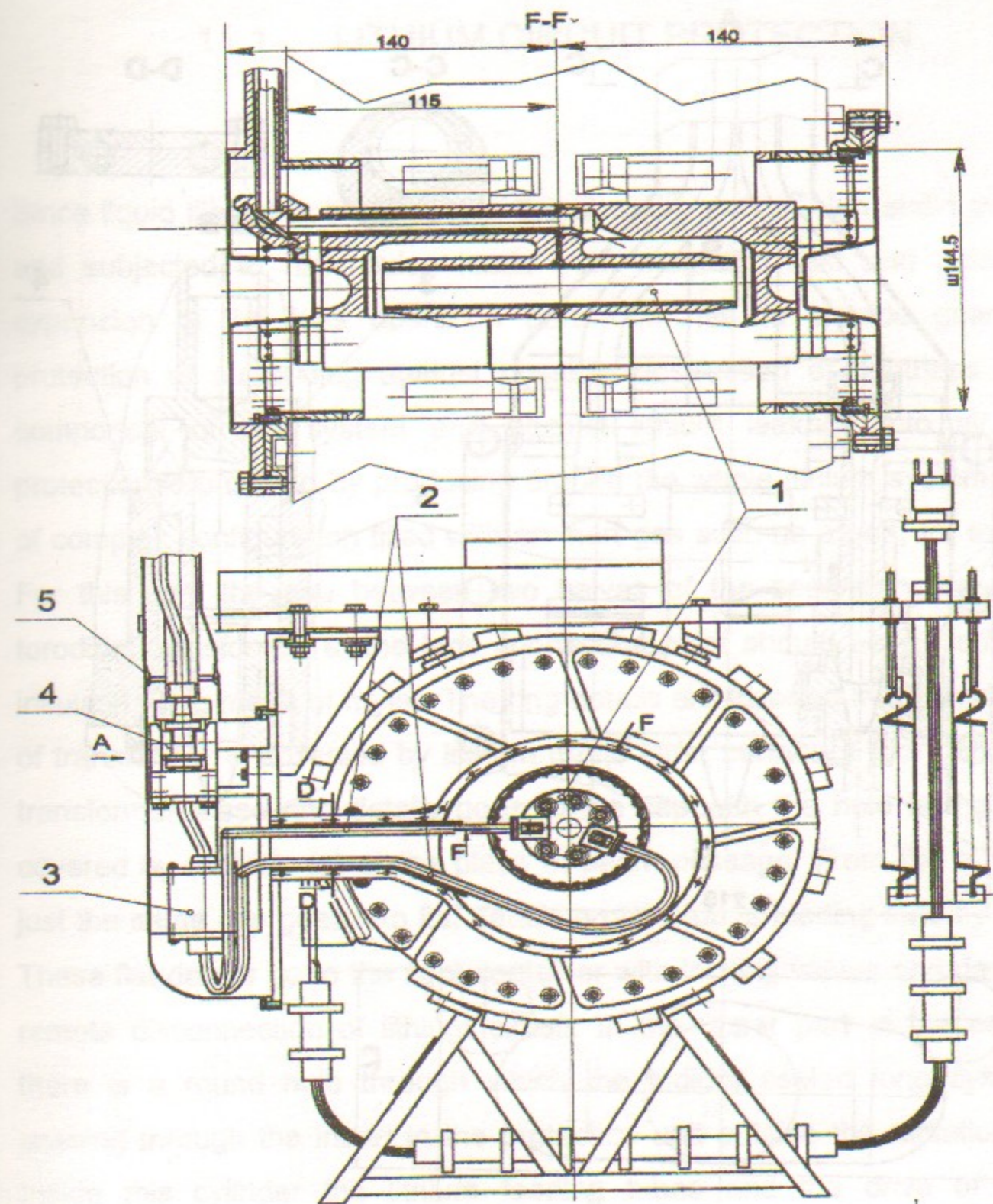


Fig. 21b. Layout of lithium in antiproton target station.  
 1-lens inside the toroidal transformer; 2-connecting tubes; 3-locking valves;  
 4-system of lithium circuit remote disconnection; 5-sealed joint lithium  
 contour protection.

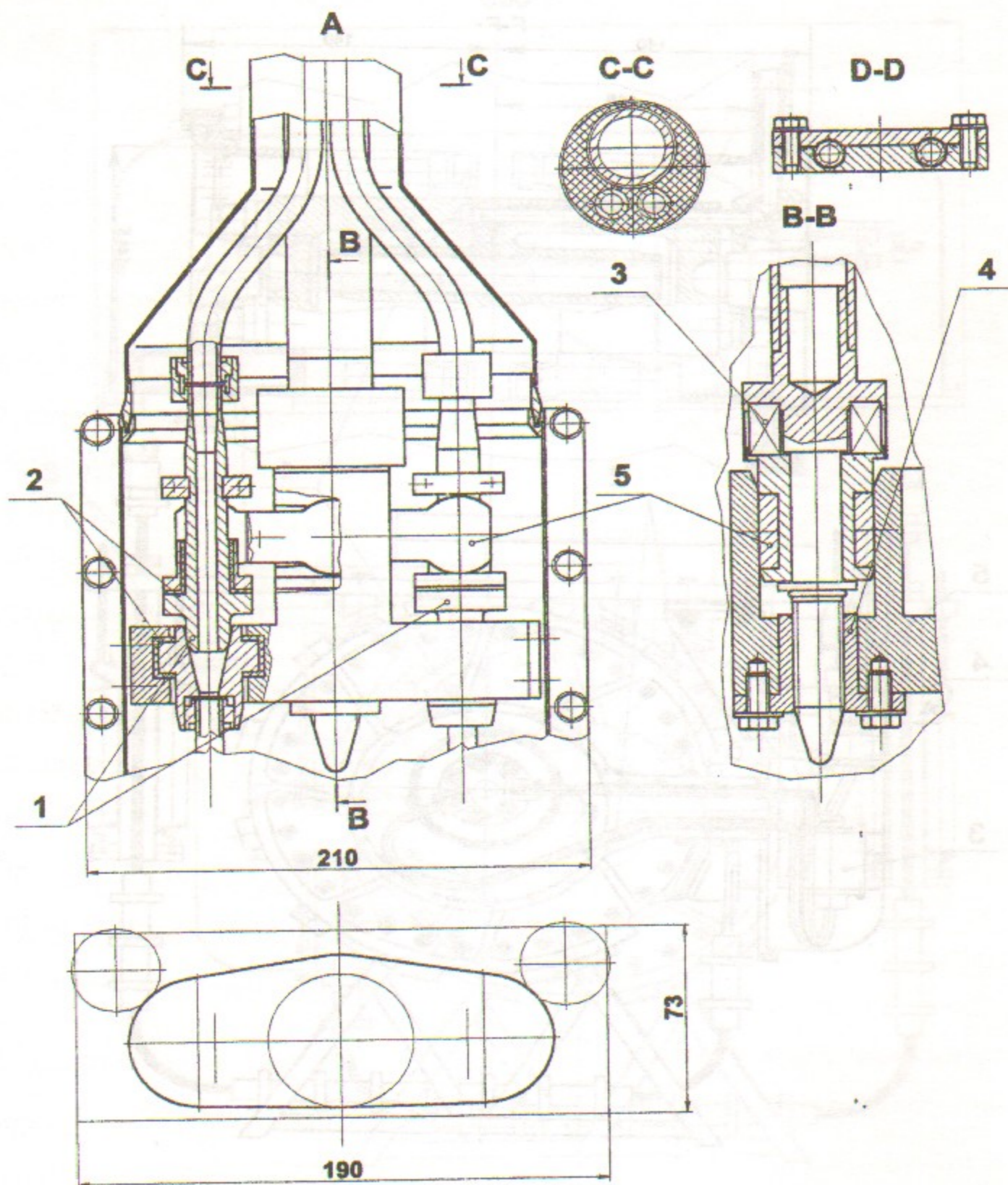


Fig.21c. Device of remote disconnection of lithium circuit.  
 1-lithium tubes joint; 2-ceramic insulation; 3-support bearing; 4-bolt with special screw; 5-pressing lever.

## 11.1 LITHIUM CIRCUIT PROTECTION

Since liquid lithium is circulating in the closed circuit at high static pressure and subjected to high pulse loads from magnetic field and pulse heat expansion of the lens operation part, one has to provide guaranteed protection of surrounding against possible destruction of tightness of any component of the system and against lithium leakage into air. Such protection is provided by producing around the whole lithium system a shell of complex configuration filled with an inert gas such as argon, for example. For this aim, the gap between two halves of the secondary turn of the toroidal transformer at the lens connection point should be closed by the insulating ring made of mylar. The ring details are inserted into cylindrical hole of transformer and sealed by indium on its inner surface. From one side of transformer these ring details go to the cap with the hole in the middle covered by titanium foil at the place of beam passage. From the other side just the same cap goes into flat details around tubes feeding lens by lithium. These flat details go to the tight container with locking valves and devices of remote disconnection of lithium circuit. In the upper part of the container there is a round hole through which the indium sealed long cylinder is passing through the insert in the protection unit outside the radiation zone. Inside this cylinder the lithium feeding tubes and the drive of remote disconnection device are located. The free space inside the cylinder is filled with the steel pellets for providing radiation protection. Beyond the protection unit the cylinder is connected with the tight container around the pump. All the joints of protective shell in the radiation zone are sealed with indium and the pump protection system can be packed with rubber. Such hermetisation of the whole lithium system allow to fill it with an inert gas with some

excessive pressure. The evidence of possible loss of tightness of the liquid-lithium circuit is indicated by the sharp decrease in the static pressure in the system.

## 12. SYSTEM HEATING AND TURN-ON

The lithium circuit components are heated up to the lithium melting temperature by different methods.

- Lens is heated by its generator operating at the lower amplitudes of current pulses and at higher rate of pulses up to  $f \approx 5 \text{ Hz}$ .

- The locking valves placed near the transformer in zone of radiation are heated by applying higher current to the exciting coils so that the valves are open.

- Long tubes connecting the pump and lens are heated by current  $\approx 300 \text{ A}$  from the conventional step-down transformer of  $\approx 3 \text{ kW}$  in power.

Since the whole system comprising lens with transformer and connecting tubes and the pump are grounded only at one point (for example, the secondary coil of the toroidal transformer), the source of heating current can be connected to ground and pump so that current will flow in parallel through both tubes.

- The pump with the heat exchanger and device for producing the static pressure will be heated by higher current flow through its exciting coils in opposite directions in each coil from special sources of current.

The heating procedure is the following:

- At the initial state at room temperature and solid lithium in the system for static pressure the zeroth pressure is established.

- The pump of water cooling circuit is off therefore there is no water circulation in the heat exchanger.

- When the heating of all components is switched on, their temperature is controlled so to establish approximately the same heating rate for separated components.

- With an increase in temperature and thermal expansion of lithium the static pressure in the system will be increased and it should be maintained on the level of a few tens of atmospheres.

- Upon melting lithium in all the components the power system of the pump is switched on in the conventional regime of alternate switching to each coil at current decrease in order to flow lithium through the system at a low rate.

- The onset of normal circulation of lithium with the design rate is indicated by the meter values of lithium flow.

- After establishing the lithium normal circulation in homogeneous distribution of temperature in all the components  $T \approx 220^\circ \text{C}$  the lens pulse generator is off and heating current for connection tubes decreases. If the power generated in the pump coils at its normal operation is sufficient for maintaining the mean temperature, the current for connecting tube heating is off.

- If the system temperature continues to grow from power generated in the pump, the water circuit pump is slowly switched on and water circulation rate is established in the heat exchanger to provide the stable temperature on the level of  $T = 200 \div 220^\circ \text{C}$ . The design static pressure of lithium is set up on the level  $P = 200 \div 300 \text{ atm}$ .

- Locking valves are switched on in the regime of normal operation synchronized with the complex cycle operation.

- After this, the system is ready for operation and lens is switched on in the normal operation regime with large current pulses.

- The power generated in lens leads to an increase in temperature of the whole lithium circuit so that water circulation rate in the heat exchanger increases up to establishing the equilibrium temperature.

The described procedure of system heating and turn-on will be computer controlled.

## REFERENCES

1. B. F. Bayanov, T. A. Vsevolozhskaya, Yu. N. Petrov and G.I. Silvestrov "The Investigation and Design Development of Lithium Lens with Large Operating Lithium Volume" Proc. of the 12th Int. Conf. of High Energy Acc. Fermilab, August 11-16, 1983, pp. 587-590
2. G. Dugan "Pbar Production and Collection at the FNAL Antiproton Source" Proc. of the 13th Int. Conf. of High Energy Acc. Novosibirsk, August 7-11, 1986, vol. 2, pp. 264-271
3. R. Bellone, A. Ijspeert, P. Sievers "The Results of Prototype Tests and Temperature and Field Computations of the CERN Lithium Lens" Proc. of the 13th Int. Conf. of High Energy Acc. Novosibirsk, August 7-11, 1986, vol. 2, pp. 272-275
4. B. F. Bayanov, T. A. Vsevolozhskaya and G. I. Silvestrov "Study of the Stresses in and Design Development of Cylindrical Lithium Lenses" Preprint BINP 84-168, Novosibirsk, 1984
5. L. D. Landau and E. M. Lifshits "Electrodynamics of continuous media" Moscow, Nauka, 1982
6. Ya. B. Zel'dovich and Yu. P. Raiser "Physics of Shock Waves and High-Temperature Hydrodynamics Phenomena, Academic Press, New York, 1967

7. T. A. Vsevolozhskaya, M. A. Lubimova and G. I. Silvestrov "Optical Properties of Cylindrical Lenses" Journal of Technical Physics, 1975, vol. XLV, N 12 ( Sov. Phys. Tech. Phys. vol. 20, N 12. Copying 1976 American Institute of Physics.)

8. T. A. Vsevolozhskaya and G. I. Silvestrov "Thermal Regime of the Cylindrical Lenses" Preprint BINP 84-100, Novosibirsk, 1984

9. B. F. Bayanov, Yu. N. Petrov and G. I. Silvestrov et al "Large Cylindrical Lenses with Solid and Liquid Lithium" EPAC, Rome, June 7-11, 1988, vol. 1, pp. 263-265.

*B. Bayanov, V. Belov, A. Chernyakin, C. Crowford,  
S. O'Day, V. Eschenko, V. Karasyuk, M. Petrichenkov,  
Yu. Petrov, G. Silvestrov, T. Sokolova, T. Vsevolozhskaya*

**Liquid lithium lens  
for Fermilab antiproton source**

Budker INP 98-23

Ответственный за выпуск А.М. Кудрявцев

Работа поступила 9.04. 1998 г.

Сдано в набор 9.04.1998 г.

Подписано в печать 9.04.1998 г.

Формат бумаги 60×90 1/16 Объем 4.6 печ.л., 3.0 уч.-изд.л.

Тираж 50 экз. Бесплатно. Заказ № 23

Обработано на IBM PC и отпечатано на

ротапринте ИЯФ им. Г.И. Будкера СО РАН

Новосибирск, 630090, пр. академика Лаврентьева, 11.